

COMPUTATIONAL STUDY OF ANTIMONY SULPHIDE ABSORBANCE
LAYER FOR SOLAR CELLS

AFIQ BIN RADZWAN

UNIVERSITI TEKNOLOGI MALAYSIA

COMPUTATIONAL STUDY OF ANTIMONY SULPHIDE ABSORBANCE
LAYER FOR SOLAR CELLS

AFIQ BIN RADZWAN

A thesis submitted in fulfilment of the
requirements for the award of the degree of
Doctor of Philosophy

Faculty of Science
Universiti Teknologi Malaysia

AUGUST 2020

ACKNOWLEDGEMENT

I would first like to extend thank **Assoc. Prof. Dr Amiruddin bin Shaari** and **Dr Rashid Ahmed**, my thesis supervisors, for giving me the opportunity to work with them and countless hours of invaluable help, critical comments and considerate guidance throughout my journey as a PhD student.

I wish to thank to Universiti Teknologi Malaysia (UTM) for providing financial support during my Ph.D study. Thank you to all the members of our research group who have provided me with a lot of helpful input. I warmly express my thanks to my family members especially my parent for all the heartfelt support they have given me the past 4 years. I also would like to thank my brother and sisters. I wish to acknowledge my fellow postgraduate and student for their continuous guidance and support.

Finally, I also wish to express my gratitude to all those who have supported and encouraged during my struggle and guided me throughout my whole study. This thesis would not have been done without the precious support of a number of remarkable peoples. My sincere thanks and deepest appreciation to all of them for being part of my Ph.D life.

ABSTRACT

The demand for cheaper, nontoxic and earth-abundant materials as absorbing layer for solar cell is immensely needed to replace scarce, toxic and expensive one. In this regard, chalcogenide materials have attracted the attention of a lot of researchers because of their great potential in different applications. Antimony sulphide (Sb_2S_3), a chalcogenide binary material is investigated to exploit its potential for different energy technologies being a less toxic, abundantly available, stable and efficient, which are the fundamentals for sustainability as well as to realize the dream of green energy. Theoretical calculations based on density functional theory (DFT) are employed to study and understand the structural, electronic and optical properties of Sb_2S_3 for three-dimensional (3-D), two-dimensional (2-D) and one-dimensional (1-D) structures. Here, the investigations have been performed by full-potential linearized augmented plane-wave method (FP-LAPW) within the WIEN2k computational code. The optical properties such as imaginary and real parts of the dielectric function, absorption coefficient, refractive index, reflectivity, and electron energy loss function are analyzed. In 3-D structure study, lattice parameters obtained are comparable to the experimental measurements. The obtained indirect energy band gap of 1.63 eV and optical properties are also closer to the experimental data. As the dimensions and size changed, the physical properties of Sb_2S_3 are also changed. The indirect energy band gaps obtained for 2-D and 1-D structures of Sb_2S_3 are 0.57 eV and 0.12 eV, respectively which are smaller than 3-D Sb_2S_3 . The investigation of thickness effect on 2-D Sb_2S_3 is presented. The obtained values of indirect energy band gaps for various levels were found to be 0.568, 0.596 and 0.609 eV for 1, 2 and 4 levels, respectively. The density of state (DOS) illustrated for both 2-D and 1-D structures are higher than 3-D structure. The obtained absorption coefficients for both Sb_2S_3 structures are around 10^4 cm^{-1} in the visible light and ultraviolet regions. The static refractive index calculated for 3-D, 2-D and 1-D structures are 3.05, 1.77 and 1.48, respectively. From these results, it is clearly shown that 2-D and 1-D Sb_2S_3 structures have lower optical properties than 3-D Sb_2S_3 . However, the absorption coefficients of 2-D and 1-D Sb_2S_3 structures are considerably higher and reflect their potentiality for photovoltaic applications.

ABSTRAK

Tuntutan bahan yang murah, tidak bertoksik dan paling banyak di Bumi sebagai lapisan penyerap di dalam sel suria adalah sangat diperlukan bagi menggantikan bahan yang susah didapati, toksik dan mahal. Berkenaan perkara ini, bahan kalkogenida telah menarik perhatian ramai penyelidik kerana potensi yang besar untuk pelbagai aplikasi tenaga. Antimoni sulfida (Sb_2S_3), bahan kalkogenida biner telah dikaji untuk mengeksploitasi potensinya untuk teknologi tenaga berbeza yang kurang toksik, senang didapati, tersedia, stabil dan cekap, yang merupakan asas kepada kelestarian dan juga untuk merealisasikan impian tenaga hijau. Pengiraan teori berdasarkan teori fungsian ketumpatan (DFT) telah digunakan untuk mengkaji dan memahami sifat-sifat struktur, elektronik dan optik Sb_2S_3 untuk struktur tiga-dimensi (3-D), dua-dimensi (2-D) dan satu-dimensi (1-D). Di sini, penyiasatan dilakukan menggunakan kaedah keupayaan penuh gelombang satah terimbuhan (FP-LAPW) dalam kod perkomputeran WIEN2K. Sifat-sifat optik seperti bahagian khayal dan nyata fungsi dielektrik, pekali penyerapan, indeks biasan, keterpantulan dan fungsi kehilangan tenaga elektron telah dianalisa. Dalam kajian struktur 3-D, dapatan parameter kekisi adalah setanding dengan pengukuran eksperimen. Dapatan jurang jalur tenaga tidak langsung 1.63 eV dan sifat optik juga hampir dengan data eksperimen. Dengan perubahan dimensi dan saiz, sifat fizikal Sb_2S_3 juga berubah. Dapatan jurang jalur tenaga tidak langsung untuk 2-D dan 1-D Sb_2S_3 masing-masing ialah 0.57 eV dan 0.12 eV yang mana ia adalah lebih kecil berbanding 3-D Sb_2S_3 . Penyiasatan kesan ketebalan ke atas 2-D Sb_2S_3 telah dibentangkan. Dapatan jurang jalur tenaga tidak langsung untuk beberapa tahap didapati 0.568, 0.596 dan 0.609 eV untuk tahap 1, 2 dan 4. Ketumpatan keadaan (DOS) yang ditunjukkan untuk kedua-dua struktur 2-D dan 1-D Sb_2S_3 adalah lebih kecil berbanding struktur 3-D. Dapatan pekali penyerapan untuk kedua-dua struktur 2-D dan 1-D Sb_2S_3 ialah dalam lingkungan 10^4cm^{-1} dalam rantau cahaya nampak dan ultraungu. Indeks biasan statik struktur 3-D, 2-D dan 1-D Sb_2S_3 yang dikira masing-masing ialah 3.05, 1.77 dan 1.48. Daripada hasil kajian, ia jelas menunjukkan struktur 2-D dan 1-D Sb_2S_3 mempunyai sifat-sifat optik yang lebih rendah berbanding 3-D Sb_2S_3 . Walau bagaimanapun, pekali penyerapan struktur 2-D dan 1-D Sb_2S_3 adalah lebih tinggi dan mencerminkan potensi mereka dalam aplikasi fotovolt.

TABLE OF CONTENTS

	TITLE	PAGE
	DECLARATION	iii
	DEDICATION	iv
	ACKNOWLEDGEMENT	v
	ABSTRACT	vi
	ABSTRAK	vii
	TABLE OF CONTENTS	viii
	LIST OF TABLES	xi
	LIST OF FIGURES	xiii
	LIST OF ABBREVIATIONS	xvi
	LIST OF SYMBOLS	xviii
	LIST OF APPENDICES	xx
CHAPTER 1	INTRODUCTION	1
	1.1 Background study	1
	1.2 Problem statements	5
	1.3 Research Objectives	7
	1.4 Research Scope	7
	1.5 Significance of Study	8
	1.6 Thesis Organization	8
CHAPTER 2	LITERATURE REVIEW	11
	2.1 Introduction	11
	2.2 Photovoltaic Solar cell	11
	2.3 Semiconductor Based-Photovoltaics Solar Cell	14
	2.4 Absorber layer in Photovoltaics Solar Cell	16
	2.5 Antimony Sulphide based Photovoltaic Cell	17
	2.5.1 Two-dimensional (2-D) Antimony Sulphide Based Photovoltaics Cell	20

2.5.2	One-Dimensional (1-D) Antimony sulphide Based Photovoltaics Cell	23
2.6	Relativistic Spin-Orbit Coupling Effect in Antimony Sulphide	25
2.7	Computational study of materials	26
2.7.1	The Quantum Many-Body Problem	29
2.7.2	The Born-Oppenheimer Approximation	30
2.7.3	The Hartree approximation	30
2.7.4	The variational principle	32
2.7.5	The Hartree-Fock approximation	33
2.7.6	Density Functional Theory	34
2.7.6.1	Hohenberg–Kohn theorems	35
2.7.6.2	The Kohn-Sham equations	36
2.7.6.3	Exchange-Correlation Functionals	38
2.7.6.4	Relativistic Spin-Orbit Coupling Effect	44
2.7.6.5	Basis Function	46
2.7.6.6	The Self-Consistent Field (SCF) procedures	51
2.7.6.7	Structural Optimization	53
2.7.6.8	Electronic Properties	53
2.7.6.9	Random Phase Approximation (RPA) and Optical Properties	56
CHAPTER 3	RESEARCH METHODOLOGY	63
3.1	Description of Methodology	63
3.2	WIEN2k package	63
3.2.1	Structural Properties Calculation	66
3.2.2	Electronic Properties Calculation	67
3.2.2.1	Density of State (DOS)	68
3.2.2.2	Band Structure	68
3.2.3	Optical Properties Calculation	69
3.3	Computational Details of Antimony Sulphide	70

CHAPTER 4	RESULTS AND DISCUSSION	77
4.1	Introduction	77
4.2	Properties of Three-Dimensional (3-D) Antimony Sulphide	77
4.2.1	Structural Properties	77
4.2.2	Electronic Properties	80
4.2.3	Optical Properties	88
4.3	Properties of Two-Dimensional (2-D) Antimony Sulphide	94
4.3.1	Electronic Properties	94
4.3.2	Optical Properties	103
4.4	Properties of One-Dimensional (1-D) Antimony Sulphide	114
4.4.1	Electronic Properties	114
4.4.2	Optical Properties	120
CHAPTER 5	CONCLUSION AND RECOMMENDATIONS	127
5.1	Conclusions	127
5.2	Recommendations	128
REFERENCES		131
LIST OF PUBLICATIONS		173

LIST OF TABLES

TABLE NO.	TITLE	PAGE
Table 2.1	Computational and experimental studies of 3-D Sb ₂ S ₃	19
Table 2.2	The experimental studies of 2-D Sb ₂ S ₃ structure-based photovoltaics solar cell.	21
Table 2.3	The experimental studies of Sb ₂ S ₃ extremely thin absorber (ETA)	23
Table 2.4	The experimental studies of 1-D Sb ₂ S ₃ .	24
Table 3.1	Crystallographic information for antimony sulphide [188].	72
Table 3.2	Thicknesses for different number of layers (from 1–8 levels) for 2-D Sb ₂ S ₃ .	73
Table 3.3	The parameters used for each structure in initialization process	75
Table 4.1	Calculated and experimental lattice constants of 3-D Sb ₂ S ₃ .	79
Table 4.2	Calculated and experimental energy gaps of 3-D Sb ₂ S ₃ .	83
Table 4.3	The band gaps of EV-GGA with and without SOC for 3-D Sb ₂ S ₃ .	84
Table 4.4	Calculated static dielectric $\epsilon_1(0)$ of 3-D Sb ₂ S ₃ for three polarization directions with different exchange-correlation potentials.	90
Table 4.5	Calculated absorption edge, $\epsilon_2(0)$ of 3-D Sb ₂ S ₃ for three polarization directions with different exchange-correlation potentials.	90
Table 4.6	Calculated refractive index, $n(0)$ of 3-D Sb ₂ S ₃ for three polarization directions with different exchange-correlation potentials.	94
Table 4.7	The band gaps of Sb ₂ S ₃ for 2-D and 3-D.	96
Table 4.8	Calculated static dielectric, $\epsilon_1(0)$ of 3-D Sb ₂ S ₃ and 2-D Sb ₂ S ₃ for EV-GGA exchange-correlation potentials.	105
Table 4.9	Calculated static refractive index, $n(0)$ of 3-D Sb ₂ S ₃ and 2-D Sb ₂ S ₃ for PBE-GGA exchange-correlation potentials.	108
Table 4.10	Static dielectric, $\epsilon(0)$ of 2-D Sb ₂ S ₃ for different levels.	110

Table 4.11	Static refractive index, $n(0)$ of 2-D Sb_2S_3 structures for different levels.	113
Table 4.12	Calculated and experimental energy gap of 1-D Sb_2S_3 and calculated energy gap of 3-D and 2-D Sb_2S_3 .	115
Table 4.13	Calculated static dielectric, $\epsilon_1(0)$ and static refractive index, $n(0)$ of 3-D Sb_2S_3 and 1-D Sb_2S_3 for EV-GGA exchange-correlation potentials.	121

LIST OF FIGURES

FIGURE NO.	TITLE	PAGE
Figure 1.1	Primary global energy consumption according to the British Petroleum Company (BP) statistical review of global energy 2017 [1]	1
Figure 1.2	Typical system of photovoltaic (PV) solar energy [16].	2
Figure 1.3	Theoretical Shockley-Queisser (S-Q) detailed-balance efficiency limit as a function of band gap [37].	4
Figure 2.1	Spectrum of solar radiation [99].	12
Figure 2.2	Schematic of a crystalline silicon (c-Si) silicon solar cell [16].	13
Figure 2.3	Photon absorption in semiconductors [130].	14
Figure 2.4	Schematic of CIGS and CdTe photovoltaic cells [136].	15
Figure 2.5	The absorption coefficient for different solar cell materials [141].	16
Figure 2.6	Schematic of absorber layer in photovoltaic cell [155].	17
Figure 2.7	Schematic of Sb ₂ S ₃ photovoltaic cells [183].	18
Figure 2.8	Sb ₂ S ₃ absorber (ETA) in a sensitized solar cell [221].	22
Figure 2.9	FESEM images of the synthesized 1-D Sb ₂ S ₃ [64].	24
Figure 2.10	Computational methods in materials study [296].	28
Figure 2.11	Partition region in unit cell according to FP-LAPW [366]	49
Figure 2.12	The flow-chart of self-consistent field (SCF) procedures for solving Kohn–Sham equations [94].	52
Figure 2.13	Energy band structure diagrams for insulators, semiconductors, and conductors [381].	54
Figure 2.14	Direct and indirect band gap of a semiconductor [381].	55
Figure 3.1	The flow of WIEN2k initialization process	64
Figure 3.2	The flow-chart for self-consistent field (SCF) procedures for WIEN2K electronic structure calculation.	66
Figure 3.3	Program flow for structure optimization in WIEN2k	67
Figure 3.4	Program flow for calculation of DOS in WIEN2k	68

Figure 3.5	Program flow for calculation of band structure in WIEN2k	69
Figure 3.6	Program flow Optics in WIEN2k.	70
Figure 3.7	Computational flow chart of antimony sulphide properties calculation using WIEN2K.	71
Figure 3.8	Crystal structure of 3-D Sb_2S_3 .	71
Figure 3.9	Crystal structure of 1 level of 2-D Sb_2S_3 with 3nm vacuum.	73
Figure 3.10	Structure of 1-D Sb_2S_3 with 30 Å vacuum at x and y direction.	74
Figure 4.1	The total energy versus volume of 3-D Sb_2S_3 using different exchange-correlation functionals.	78
Figure 4.2	Special symmetry directions used to plot the band structure in first Brillouin zone for the orthorhombic Sb_2S_3 .	80
Figure 4.3	Energy band structure of 3-D Sb_2S_3 according to different exchange-correlation potentials.	81
Figure 4.4	Band structure of EV-GGA with and without SOC for 3-D Sb_2S_3 .	84
Figure 4.5	Total DOS and total DOS of atoms Sb and S of 3-D Sb_2S_3 according to different exchange-correlation potentials.	86
Figure 4.6	Partial DOS of 3-D Sb_2S_3 according to different exchange-correlation potentials.	87
Figure 4.7	Dielectric function, $\epsilon(\omega)$ of 3-D Sb_2S_3 according to different exchange-correlation potentials.	89
Figure 4.8	Absorption coefficient, $\alpha(\omega)$ and energy loss, $L(\omega)$ for 3-D Sb_2S_3 according to different exchange-correlation potentials	92
Figure 4.9	Reflectivity, $R(\omega)$ and refractive index, $n(\omega)$ for 3-D Sb_2S_3 according to different exchange-correlation potentials.	93
Figure 4.10	Band structure of 2-D Sb_2S_3 for LDA, PBE-GGA, EV-GGA and EV-GGA with SOC.	95
Figure 4.11	Total of 3-D and 2-D for Sb_2S_3 .	98
Figure 4.12	Total DOS of the Sb and S atoms of the 2-D Sb_2S_3 .	99
Figure 4.13	Partial DOS of the 2-D Sb_2S_3 .	100

Figure 4.14	Band structures of the 3-D Sb_2S_3 (a) and 2-D Sb_2S_3 with five different thicknesses: 1 level (b), 2 levels (c), 3 levels (d), 4 levels (e), 5 levels(f).	101
Figure 4.15	The illustration of total density of states for the 2-D Sb_2S_3 with various thickness.	102
Figure 4.16	The real parts of the dielectric function, $\varepsilon_1(\omega)$ for 2-D Sb_2S_3 .	103
Figure 4.17	The calculated imaginary parts of the dielectric function $\varepsilon_2(\omega)$ for 2-D Sb_2S_3 .	104
Figure 4.18	Calculated absorption coefficient, $\alpha(\omega)$ of 2-D Sb_2S_3 .	106
Figure 4.19	Calculated energy-loss $L(\omega)$ of 2-D Sb_2S_3 .	107
Figure 4.20	Calculated refractive index $n(\omega)$ of 2-D Sb_2S_3 .	107
Figure 4.21	Calculated reflectivity $R(\omega)$ of 2-D Sb_2S_3 .	109
Figure 4.22	The real parts of the dielectric function, $\varepsilon_1(\omega)$ for different levels of 2-D Sb_2S_3 .	110
Figure 4.23	The imaginary part of the dielectric function, $\varepsilon_2(\omega)$ for different levels of 2-D Sb_2S_3 .	111
Figure 4.24	The absorption coefficient, $\alpha(\omega)$ for different levels of 2-D Sb_2S_3 .	112
Figure 4.25	The refractive index, $n(\omega)$ for different levels of 2-D Sb_2S_3 structures.	113
Figure 4.26	The band structure of Sb_2S_3 (a) 3-D and (b) 1-D.	114
Figure 4.27	The band structure of 1-D Sb_2S_3 with (red line) and without the inclusion of SOC (blue line)	117
Figure 4.28	Total DOS of the 1-D Sb_2S_3 .	118
Figure 4.29	Partial DOS of the 1-D Sb_2S_3 .	119
Figure 4.30	The real part, $\varepsilon_1(\omega)$ of dielectric function for 1-D (a) and 3-D (b) of Sb_2S_3 .	120
Figure 4.31	The imaginary parts $\varepsilon_2(\omega)$ of dielectric function for 1-D (a) and 3-D (b) structure of Sb_2S_3 .	121
Figure 4.32	The calculated absorption coefficient, $\alpha(\omega)$ of 1-D Sb_2S_3 .	122
Figure 4.33	The calculated refractive index, $n(\omega)$ of 1-D Sb_2S_3 .	123
Figure 4.34	The calculated reflectivity, $R(\omega)$ of 1-D Sb_2S_3 .	124
Figure 4.35	The calculated energy-loss, $L(\omega)$ of 1-D Sb_2S_3	125

LIST OF ABBREVIATIONS

1-D	- One-Dimension
2-D	- Two-Dimensional
3-D	- Three-Dimensional
AlN	- Aluminium Nitride
a-Si	- Amorphous Silicon
BeO	- Beryllium Oxide
Bi ₂ S ₃	- Bismuthinite
Bi ₂ Se ₃	- Guanajuatite
BZ	- Brillouin Zone
CdTe	- Cadmium Telluride
CIGS	- Copper Indium Gallium Diselenide
CO ₂	- Carbon Dioxide
c-Si	- Crystalline Silicon
DOS	- Density of State
DSCs	- Dye-Sensitized Cells
ETA	- Extremely Thin Absorber
EV-GGA	- Engel Vosko Generalized Gradient Approximation
FP	- Full Potential
FP-LAPW	- Full Potential Augmented Plane Wave
FTO	- Fluorine-doped Tin Oxide
GaP	- Gallium Phosphide
GaS	- Gallium Sulfide
GaSe	- Gallium Selenide
GWA	- GW Approximation
HF	- Hartree-Fock
HK	- Hohenberg–Kohn
LDA	- Local Density Approximation
MT	- Muffin Tin
PBE-GGA	- Perdew–Burke–Ernzerhof Parameterized Generalized Gradient Approximation

PBEsol-GGA	-	Perdew-Burke Ernzerhof Parameterized Generalized Gradient Approximation for Solids and Surfaces
PCE	-	Power Conversion Efficiency
PV	-	Photovoltaic
RPA	-	Random phase approximation
Sb ₂ S ₃	-	Antimony Sulphide
Sb ₂ Se ₃	-	Antimonselite
SCF	-	Self-Consistent Field
SOC	-	Spin Orbit Coupling
TB-mBJ	-	Tran-Blaha-Modified-Becke-Johnson
WC-GGA	-	Wu-Cohen Parameterized Generalized Gradient Approximation
ZnO	-	Zinc Oxide

LIST OF SYMBOLS

h	-	Planck's constant
μm	-	Micrometer
eV	-	Electron volt
cm^{-1}	-	Centimeter per ssecond
α	-	Absorption coefficient
nm	-	Nanometer
PPM	-	Parts per million
%	-	Percentage
Ψ	-	Schrödinger wavefunction
Φ	-	Electronic wavefunction
H	-	Hamiltonian
N	-	Number of atoms
m_i	-	Nuclei mass
m_e	-	Electron mass
\vec{R}_i	-	Nuclei position
\vec{r}_i	-	Electron position
e	-	Electron charge
Z	-	Atomic number
\hat{T}	-	Kinetic energy of electron
\hat{T}_n	-	Kinetic energy of nuclei
\hat{V}_{ee}	-	Coulomb interaction of electron-electron
\hat{V}_{ext}	-	Coulomb interaction of electron-nucleus
\hat{V}_{nn}	-	Coulomb interaction of nucleus-nucleus
E	--	Total energy
E_{elec}	-	Nuclear energy
E_{nuc}	-	Electronic energy
E_H	-	Hartree energy
ρ	-	Electron density
ρ_0	-	Electron ground-state density,

E_0	-	Ground-state energy
E_{KS}	-	Kohn-sham energy
ε_{XC}	-	Exchange correlation energy density
V_{XC}	-	Exchange correlation potential
V_{eff}	-	Effective potential
V_H	-	Hartree potential
\hat{H}_{KS}	-	Kohn-sham hamiltonian
C_k^i	-	Coefficient of basis set
E_{XC}^{RPA}	-	Random phase approximation (RPA) exchange-correlation energy
ε_1	-	Real part of dielectric function
ε_2	-	Imaginary part of dielectric function
k	-	Reciprocal vector in brillouin zone
G	-	Reciprocal lattice vector
V_{cell}	-	Volume of unit cell
ρ_{in}	-	Initial electron density
ρ_{out}	-	Output electron density
$V_{x,\sigma}^{BJ}$	-	Becke-Johnson (BJ) exchange potential
$V_{x,\sigma}^{BR}$	-	Becke-Roussel (BR) exchange potential
$V_{x,\sigma}^{mBJ}$	-	Modified Becke-Johnson exchange potential
\hat{H}_{SO}	-	Spin -orbit coupling hamiltonian
V_0	-	Equilibrium volume
B_0	-	Bulk modulus
B_1	-	First derivative of the bulk modulus with respect to pressure
P	-	Principal value of the integral in irreducible brillouin zone
ω	-	Frequency
n	-	Refractive index
R	-	Reflectivity
L	-	Loss function

LIST OF APPENDICES

APPENDIX	TITLE	PAGE
Appendix A	Structure file for Bulk antimony Sulphide	169
Appendix B	Convergence Test of Vacuum layer	171

CHAPTER 1

INTRODUCTION

1.1 Background study

In the modern civilization, most of the global energy is produced from fossil fuels [1] mainly petroleum, natural gas and coal as described in Figure 1.1.

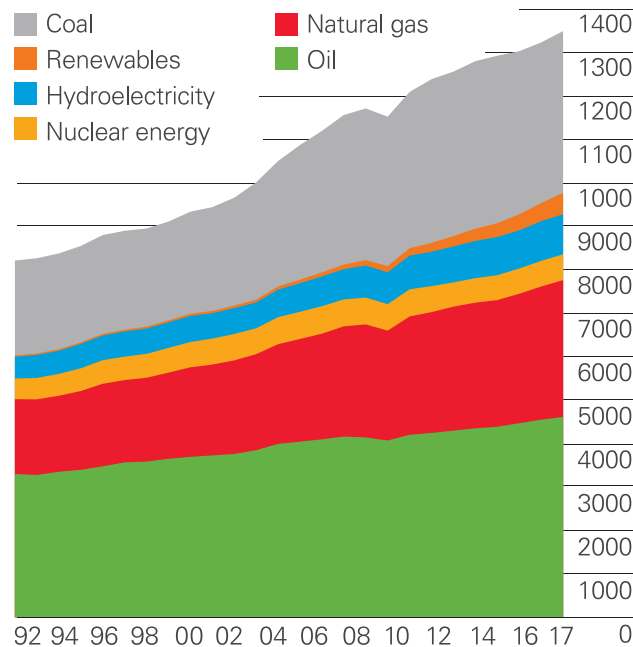


Figure 1.1 Primary global energy consumption according to the British Petroleum Company (BP) statistical review of global energy 2017 [1]

Unfortunately, the civilization's overuse leading to the rapid depletion of global energy resource supplies. The global energy consumption is expected to be increased at the rate of 1.5% [2]. Global consumption of fossil fuels increased 24% for coal, 20% for natural gas and 7.5% for petroleum from 2005 to 2014 [3]. Fossil fuels are also harmful for the environment. Emissions of carbon dioxide (CO₂) from the fossil fuel power plants are not only affecting the climate [4], but they also destroy wild habitats [5] and cause pollution problems [6], as well as serious human health

problems [7]. In 2017, global CO₂ emission from fossil fuels has risen by 1.6% and it is expected to go up by more than 2% in 2018 [8,9]. Considering energy is very important to modern society, therefore it is very important to find alternative energy resource such as renewable energy to satisfy the world sustainable and clean energy demand [10]. In 2017, global investors around the world invested 279.8 billion USD in the development of renewable energy technologies [11].

Among renewable resources, solar energy has great potential for sustainable and clean energy production due to its abundance and free of CO₂ emission [12]. Installation of 113,533 household solar cells in California, USA, have reduced 696,544 metric tons of CO₂ emissions [13]. According to M. Hosenuzzaman, et al. [14], the use of solar cells can lower 69–100 million tons of CO₂ by 2030. The Sun emits solar energy at a rate of about 3.8×10^{26} kW [12]. This energy can be harvested with solar cell [15]. Solar cells are devices that convert photon energy of sunlight into useful electricity. Schematic system of photovoltaic (PV) solar energy is shown in Figure 1.2.

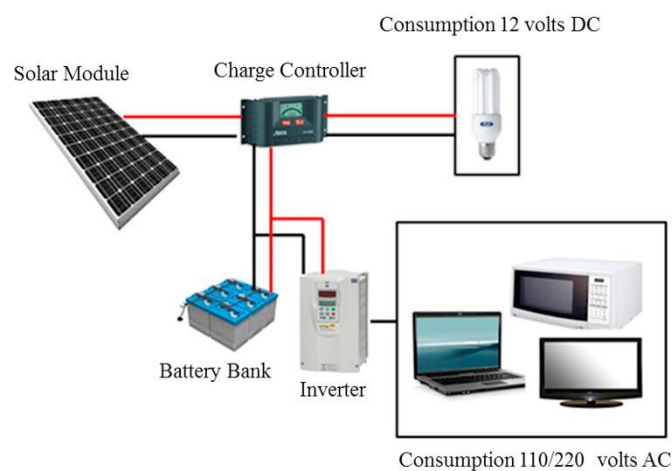


Figure 1.2 Typical system of photovoltaic (PV) solar energy [16].

Solar cells based on semiconductor have shown great performance due to its unique physical properties. The first generation of solar cells were developed based on semiconductor crystalline silicon (c-Si) [17] and gallium arsenide (GaAs) [18]. The first generation of solar cells are wafer-based solar cell. However, GaAs are too expensive for terrestrial large-area applications because of the availability of rare of gallium (Ga) element. The average estimated crustal abundance of gallium is generally

less than 19 parts per million (ppm) [19]. Currently c-Si based solar cells have dominated solar cell market because of their performance. In 2017, crystalline silicon solar cells have dominated around 95% of the solar market [20]. As well understood silicon is, non-toxic, earth-abundant and stable. Note that natural abundance of Si is 25.7 ppm which much higher than Ga [21]. However, due its complex process of purifying for solar-grade silicon from its raw source made the production expensive [22]. The cost of pure crystalline silicon is about 40-60% of the solar cell manufacturing cost. Average manufacturing cost of a silicon-based solar cell is \$0.38 per watt and selling price of \$0.44 per watt in 2015 [23]. To install solar power at large scales, huge plots of land are often required. About 16,187 m² of land area would require for a 1MW solar power plant [24].

In the search for cost reduction for solar cells, second-generation solar cell has been developed as absorber layer in solar cells. Currently, Amorphous silicon (a-Si) [25], cadmium Telluride (CdTe) [26], and copper indium gallium diselenide (CIGS) [27] are the leading materials in second generation solar cells. These materials have higher absorption than crystalline silicon (c-Si) [28,29] and close to the ideal material for photovoltaic conversion. These types of solar cells are considered as the second generation of solar cell. However, until now, c-Si solar cell has the highest power conversion efficiency (PCE) [30]. As shown in Figure 1.3, the higher efficiency solar cells are GaAs and c-Si. The efficiency of CdTe and CIGS are 21.0 % and 21.7 % respectively [30]. The major factor that contributing to this issue is the band gap of the semiconductor material. c-Si has a nearly ideal band gap (1.34 eV) [31] to absorb the maximum photons from the sun's radiation [32]. Currently, second generation solar cell may suffer from issues of availability [33] and toxicity [34] ,if widely used. The estimated crustal abundance of cadmium (Cd), indium (In), tellurium (Te) and selenium (Se) are 0.098 ppm, 0.05 ppm, 0.001 ppm and 0.05 ppm respectively [35]. Hence, the price of these materials has increased because of their low abundance in the earth's crust. The price of Cd, In, Te and Se are 100 \$/kg, 700 \$/kg, 168 \$/kg and 300 \$/kg respectively [35]. The In materials are the most expensive due to its application in liquid crystal display (LCD) screen technology. The toxicity of thin film solar cells came from cadmium (Cd). Cadmium poisoning is one of the global health problems that affect many organs and it can cause deaths. Long-term exposure to cadmium can leads to organ system toxicity and cancer [36].Hence, Cadmium based

technologies should be restricted to a minimal or no harmful level. Thus, alternative materials for solar cell which are cheaper, abundant, and less toxic need to be developed.

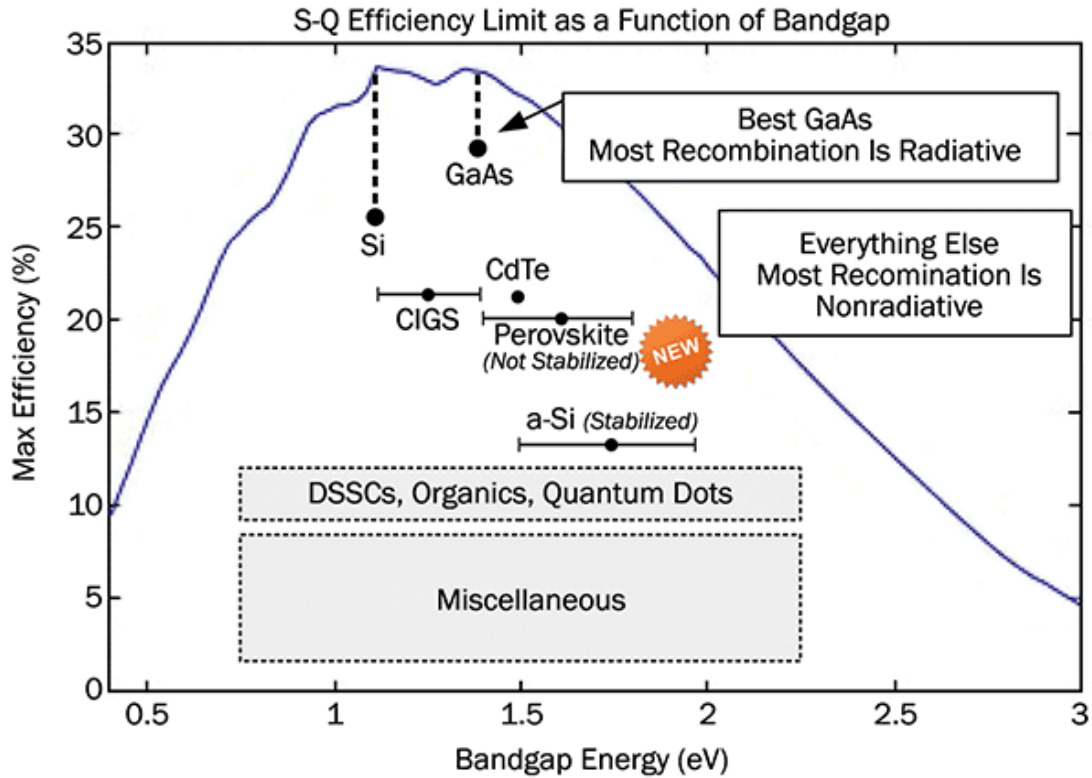


Figure 1.3 Theoretical Shockley-Queisser (S-Q) detailed-balance efficiency limit as a function of band gap [37].

Third generation of solar cell [38] was developed to overcome the issues in first- and second-generation solar cells. Third-generation solar cells usually refer to technologies that promise to be even cheaper than previous generations. Third-generation solar cells include organic materials, dye-sensitized solar cells (DSSCs) and perovskite solar cell. However, third-generation solar cells are still in development and not been widely marketed. The efficiency of third generation solar cells are between 9.7% to 20.9% [30]. DSSCs are formed by porous layer of titanium dioxide (TiO_2) nanoparticles (inorganic), covered with a molecular dye (organic) that absorbs photon [39]. The highest efficiency has been reported so far is only 11.9% [30]. However, organic molecular dye used suffers instability problems. Instead of using a molecular dye, extremely thin absorber (ETA) layer of a small band gap semiconductor can be used as absorber [40]. The efficiency of 4.9% has been achieved [41]. However,

semiconductor sensitized solar cells (SSSC) are much less reported than the DSSC but are attracting increasing interest. Some researchers consider other semiconductor as the alternative to TiO_2 such as (1 dimensional) 1-D zinc oxide (ZnO) [42] and 1-D Si [43]. The efficiency of 1-D ZnO and 1-D Si are 7.13% and 0.253%. However, these efficiencies are not high enough for commercial application.

Sham L.J. [44] and Xiao H. [45] have shown that the computational method density functional theory (DFT) is a suitable method in calculating the electronic structure of semiconductor materials. DFT has been used to study material for solar cell application such c-Si [46], CdTe [47] and CIGS [48]. Recent years, DFT has been used to study low-dimensional structure [49–51].

1.2 Problem statements

Several material candidates from chalcogenide group compound materials such as CdTe and CIGS are promising materials for photovoltaic applications, because of their appropriate energy gaps and photoconductive properties [52]. Among the metal chalcogenides group which a semiconductor material, antimony sulphide (Sb_2S_3) has gained intensive research for optoelectronic devices in various form. Sb_2S_3 satisfied the requirement future generation of solar cells. Due to strong optical properties, Sb_2S_3 is suitable 2-D solar cell [53–61]. However, their PCE is not high as other commercial solar cells [62]. Several studies found that Sb_2S_3 extremely thin absorber has shown the most encouraging results to replace photoactive dyes in dye-sensitized solar cells [53,63–65]. The highest solar cell efficiency obtained for DSSCs is 7.5% [30]. However, the band gaps obtained are varied due to the fabrication methods used. From the literatures, Sb_2S_3 have good electrical properties [66–73]. Sb_2S_3 are among several candidates to be considered as replacement of TiO_2 in DSSC [74]. Many physical properties exhibit strong dependence on their size and dimensionality [75,76]. However, this effect is rarely reported due to limited study on Sb_2S_3 and some optical properties also are not revealed. Thus, optical properties of Sb_2S_3 are not well understood. 1-D Sb_2S_3 shows a small band gap closer to ideal band gap for solar cell material compared to its other forms. The potential of Sb_2S_3 as

absorber in for photovoltaic (PV) solar cell is unclear due to the challenge and limitation in experimental study.

There are areas in material studies that are not accessible by experiment such as the electronic structure. In spite of the various applications proposed for Sb_2S_3 , very little is known of its electronic structure. It is well recognized that the electronic structure of solids plays a very effective tool in determining their properties [77]. Density functional theory (DFT) has been well used for investigating electronic structure in semiconductor [44,45]. There are numerous computational studies of 3-D Sb_2S_3 using DFT that have been done [78,79,88,80–87] but there are only several studies reported on the optical behaviour of this compound. Hence, relationship between electronic structure and optical properties are not well understood. Moreover, the computational study on low dimensional Sb_2S_3 such as 2-D and 1-D structures are highly rare so far due to its complex and disordered structure. There are only two theoretical studies on low dimensional Sb_2S_3 [79,86]. However, Chen, J.H. et al. did not calculate the optical properties and Caruso, F. et al. did not present the density of state (DOS) which both are essential for optoelectronic application study. Thus, the effects of dimensionality reduction on electronic structure are unclear. Some experimental studies [89,90] observed the changes in physical properties of 2-D Sb_2S_3 with changes in thickness. However, the thickness dependence in Sb_2S_3 has not been discussed theoretically. Hence, the study of electronic structure for different structure of Sb_2S_3 is critical. There are numerous exchange correlation approximations have been proposed to enhance the accuracy of DFT calculation [91,92]. However, only a few exchange correlation approximations have been used in DFT calculations of Sb_2S_3 . The performance of exchange correlation approximation on optical properties of Sb_2S_3 also unclear.

The spin-orbit coupling (SOC) in DFT calculation is usually ignored due to the small effect but, it is substantial. For heavy element such as antimony (Sb). However, there is not very much study regarding to this matter. Currently, only two DFT studies on Sb_2S_3 has been done with inclusion of SOC [82,86]. However, that is only in 3-D level. The SOC effect is different for each dimensional structure [93]. The effect of SOC in low dimensional Sb_2S_3 structure is unknown.

1.3 Research Objectives

To resolve the above-mentioned issues, this study embarks on the following objectives:

- (a) To calculate the electronic and optical properties of Sb_2S_3 using different approximations.
- (b) To determine the effect of thickness in electronic and optical properties of Sb_2S_3 .
- (c) To determine the effect of spin orbit coupling (SOC) in electronic band gap of Sb_2S_3 .
- (d) To identify the potential of Sb_2S_3 as absorber in photovoltaic (PV) solar cell.

1.4 Research Scope

The investigation of the structural, electronic and optical properties in three-dimensional (3-D), two-dimensional (2-D) and one-dimensional (1-D) of Sb_2S_3 structures will be performed using a computational method based on DFT [94–96]. The 3-D, 2-D and 1-D structures are included in this study. The WIEN2k code [97–101] based on full potential augmented plane wave (FP-LAPW) methodology will be used to analyse structural, electronic, and optical properties of each structure. The spin orbit coupling is included for 3-D, 2-D and 1-D structures calculations.

Investigation of the structural optimization of 3-D Sb_2S_3 is carried out by employing local density approximation (LDA), Engel Vosko generalized gradient approximation (EV-GGA), Perdew-Burke-Ernzerhof parameterized generalized gradient approximation (PBE-GGA), Wu-Cohen parameterized GGA (WC-GGA) and Perdew-Burke Ernzerhof parameterized generalized gradient approximation for solids and surfaces (PBEsol-GGA) exchange correlation functional. But the investigation of the electronic and optical properties of 3-D Sb_2S_3 are carried out by employing above-

mentioned exchange-correlation functionals with addition of Tran-Blaha-modified-Becke-Johnson (TB-mBJ).

Computational study on 2-D and 1-D Sb_2S_3 structures are carried out using optimized unit cell from 3-D calculation. The investigation electronic and optical of 2-D Sb_2S_3 with thickness of 1 level (1.16 nm) is carried out using LDA, PBE-GGA, EV-GGA. However, thickness effect study on 2-D Sb_2S_3 is carried out using EV-GGA only. The thickness is increased from 1 to 8 levels. For 1-D Sb_2S_3 , the investigation of electronic and optical of with diameter of several nanometers is carried out using EV-GGA.

1.5 Significance of Study

The successful execution of this FP-LAPW method can open avenues for designing the novel materials, and moreover, can provide a guideline to the industrial sector for synthesizing cost-effective novel materials for energy efficient technologies and save energy thus provide a safe environment. Furthermore, DFT provide the properties that cannot reach by experimental method. Additionally, this study reveals much clear optical properties of Sb_2S_3 explain the relationship between electronic structure and optical behaviour. Besides, the intention of this study is to present the accurate procedure of first principles to calculate the electronic structure in low-dimensional structure level. However, due to the limit of computation, the physical properties of Sb_2S_3 in various form cannot be explored widely. Furthermore, the properties studied in this project is limited. However, results obtained are enough to give proper understanding the effect of dimensionality and size reduction. These efforts hoped can stimulate more research on solar cell materials.

1.6 Thesis Organization

This thesis is categorized into five different chapters. Chapter 1 describes the importance of harvesting solar energy and solar cell technology. Furthermore, the

problem statements, research objectives, scope of research, significance of study and thesis organization are defined in this chapter. Chapter 2, the overview of the literature related to the research title. This chapter covers fundamental of solar cell, the experimental and theoretical studies on Sb_2S_3 and lastly DFT method. Next, the Chapter 3 provides the details of WIEN2K package and procedure of calculation.as well as the detail of calculation for 2-D and 1-D Sb_2S_3 structures. Chapter 4 discusses the structural, electronic and optical properties of 3-D Sb_2S_3 . The effect of SOC is also included in this chapter as well as the detailed discussion for electronic and optical of 2-D and 1-D Sb_2S_3 structures. The effect of thickness on 2-D Sb_2S_3 is also discussed in the end of this chapter. Finally, in the Chapter 5, the general conclusion along with recommendation are discussed. At the end of thesis, the list of reference and appendix are presented.

REFERENCES

1. British Petroleum. BP Statistical Review of World Energy 2017. British Petroleum. 2017.
2. Ali N, Hussain A, Ahmed R, Wang M, Zhao C, Haq BU, et al. Advances in nanostructured thin film materials for solar cell applications. *Renew Sustain Energy Rev*, 2016,59:726–737.
3. Covert T, Greenstone M, Knittel CR. Will We Ever Stop Using Fossil Fuels? *J Econ Perspect*, 2016,30(1):117–138.
4. Bulkeley H, Newell P. *Governing climate change*. Routledge, 2015.
5. Dale VH, Parish ES, Kline KL. Risks to global biodiversity from fossil-fuel production exceed those from biofuel production. *Biofuels, Bioprod Biorefining*, 2015,9(2):177–189.
6. Jacobson MZ. *Air Pollution and Global Warming: History, Science, and Solutions*. Cambridge university press, 2012.
7. Perera F. Multiple threats to child health from fossil fuel combustion: impacts of air pollution and climate change. *Environ Health Perspect*, 2016,125(2):141–148.
8. Le Quéré C, Andrew RM, Friedlingstein P, Sitch S, Hauck J, Pongratz J, et al. Global Carbon Budget 2018. *Earth Syst Sci Data*, 2018,10(4):2141–2194.
9. Figueres C, Quéré C Le, Mahindra A, Bäte O, Whiteman G, Peters G, et al. Emissions are still rising: ramp up the cuts. *Nature*, 2018,564(7734):27–30.
10. Orr FM. Addressing Climate Change with Clean Energy Technology. *ACS Energy Lett*, 2016,1(1):113–114.
11. Cuming V, Mills L, Strahan D, Boyle R, Stopforth K, Latimer S, et al. Global Trends in Renewable Energy Investment 2018. 2018.
12. Kannan N, Vakeesan D. Solar energy for future world: - A review. *Renew Sustain Energy Rev*, 2016,62:1092–1105.
13. Arif MS. Residential Solar Panels and Their Impact on the Reduction of Carbon Emissions Mashail S. Arif. In: *Spring*. 2013: 1–18.
14. Hosenuzzaman M, Rahim N, Selvaraj J, Hasanuzzaman M, Malek ABMA, Nahar A. Global prospects, progress, policies, and environmental impact of

- solar photovoltaic power generation. *Renew Sustain Energy Rev*, 2015,41:284–297.
15. Bhatia SC. *Advanced renewable energy systems*. 2014.
 16. Sampaio PGV, Gonzi M, Lez MOA. Photovoltaic solar energy: Conceptual framework. *Renew Sustain Energy Rev*, 2017,74:590–601.
 17. Chapin DM, Fuller CS, Pearson GL. A New Silicon p-n Junction Photocell for Converting Solar Radiation into Electrical Power. *J Appl Phys*, 1954,25(5):676–677.
 18. Knechtli R., Loo R., Kamath G. High-efficiency GaAs solar cells. *IEEE Trans Electron Devices*, 1984,31(5):577–588.
 19. Schulz K, DeYoung J, Seal R, Bradley D. *Critical Mineral Resources of the United States: Economic and Environmental Geology and Prospects for Future Supply*. Geological Survey, 2018.
 20. Sinke WC. Development of photovoltaic technologies for global impact. *Renew Energy*, 2019,138:911–914.
 21. Haynes WM. *CRC handbook of chemistry and physics*. 2014.
 22. Mauk MG. Silicon solar cells: Physical metallurgy principles. *JOM*, 2003,55(5):38–42.
 23. Sharma A, Shafer W. Top solar power industry trends for 2015. 2015 doi:10.1007/s13398-014-0173-7.2.
 24. Perpiña C, Batista F, Lavalle C. An assessment of the regional potential for solar power generation in EU-28. *Energy Policy*, 2016,88:86–99.
 25. Carlson DE, Wronski CR. Amorphous silicon solar cell. *Appl Phys Lett*, 1976,28(11):671–673.
 26. Cusano DA. CdTe solar cells and photovoltaic heterojunctions in II–VI compounds. *Solid State Electron*, 1963,6(3):217–232.
 27. Hahn H, Frank G, Klingler W, Störger AD, Störger G. Untersuchungen über ternäre Chalkogenide. VI. Über Ternäre Chalkogenide des Aluminiums, Galliums und Indiums mit Zink, Cadmium und Quecksilber. *Zeitschrift für Anorg und Allg Chemie*, 1955,279(5–6):241–270.
 28. Lee TD, Ebong AU. A review of thin film solar cell technologies and challenges. *Renew Sustain Energy Rev*, 2017,70:1286–1297.
 29. Escoubas L, Simon JJ, Le Rouzo J, Bermudez V. Innovative approaches in thin film photovoltaic cells. In: *Optical Thin Films and Coatings*. Woodhead

- Publishing, 2013: 596–630.
30. Green MA, Hishikawa Y, Dunlop ED, Levi DH, Hohl-Ebinger J, Ho-Baillie AWY. Solar cell efficiency tables (version 51). *Prog Photovoltaics Res Appl*, 2018,26(1):3–12.
 31. Peter LM. Towards sustainable photovoltaics: the search for new materials. *Philos Trans R Soc A Math Phys Eng Sci*, 2011,369(1942):1840–1856.
 32. Nguyen HT, Rougieux FE, Mitchell B, Macdonald D. Temperature dependence of the band-band absorption coefficient in crystalline silicon from photoluminescence. *J Appl Phys*, 2014,115(4):043710.
 33. Helbig C, Bradshaw AM, Kolotzek C, Thorenz A, Tuma A. Supply risks associated with CdTe and CIGS thin-film photovoltaics. *Appl Energy*, 2016,178:422–433.
 34. Jaffe R, Price J. Energy Critical Elements. *Mater Res Soc*, 2011.
 35. Vigil-Galán O, Courel M, Andrade-Arvizu JA, Sánchez Y, Espíndola-Rodríguez M, Saucedo E, et al. Route towards low cost-high efficiency second generation solar cells: current status and perspectives. *J Mater Sci Mater Electron*, 2015,26(8):5562–5573.
 36. Rafati Rahimzadeh M, Rafati Rahimzadeh M, Kazemi S, Moghadamnia A-A. Cadmium toxicity and treatment: An update. *Casp J Intern Med*, 2017,8(3):135–145.
 37. Coffey VC, Writer S. Next-Generation Solar Technology : Thin Is In. *Photonics Spectra*, 2015,49(11):36–39.
 38. Jean J, Brown R, Jaffe RL, Buonassisi T, Bulovic V, Brown PR, et al. Pathways for Solar Photovoltaics Joel. *Energy Environ Sci*, 2015,8(4):1200–1219.
 39. Sugathan V, John E, Sudhakar K. Recent improvements in dye sensitized solar cells: A review. *Renew Sustain Energy Rev*, 2015,52:54–64.
 40. Lévy-Clément C. Nanostructured ETA-Solar Cells. In: *Nanostructured Materials for Solar Energy Conversion*. Elsevier, 2006: 447–484.
 41. Huerta-Flores AM, García-Gómez NA, de la Parra-Arciniega SM, Sánchez EM. Fabrication and characterization of a nanostructured TiO₂/In₂S₃-Sb₂S₃/CuSCN extremely thin absorber (eta) solar cell. *Semicond Sci Technol*, 2016,31(8):085011.
 42. Yang Y, Zhao J, Cui C, Zhang Y, Hu H, Xu L, et al. Hydrothermal growth of

- ZnO nanowires scaffolds within mesoporous TiO₂ photoanodes for dye-sensitized solar cells with enhanced efficiency. *Electrochim Acta*, 2016,196:348–356.
43. Hsieh Y-D, Lee M-W, Wang G-J. Sb₂S₃ Quantum-Dot Sensitized Solar Cells with Silicon Nanowire Photoelectrode. *Int J Photoenergy*, 2015,2015:1–10.
 44. Sham LJ, Schlüter M. Density-Functional Theory of the Energy Gap. *Phys Rev Lett*, 1983,51(20):1888–1891.
 45. Xiao H, Tahir-Kheli J, Goddard WA. Accurate Band Gaps for Semiconductors from Density Functional Theory. *J Phys Chem Lett*, 2011,2(3):212–217.
 46. Dal Corso A, Pasquarello A, Baldereschi A, Car R. Generalized-gradient approximations to density-functional theory: A comparative study for atoms and solids. *Phys Rev B - Condens Matter Mater Phys*, 1996,53(3):1180–1185.
 47. Dal Corso A, Resta R, Baroni S. Nonlinear piezoelectricity in CdTe. *Phys Rev B*, 1993,47(24):16252–16256.
 48. Chen XD, Chen L, Sun QQ, Zhou P, Zhang DW. Hybrid density functional theory study of Cu(In_{1-x}Ga_x)Se₂ band structure for solar cell application. *AIP Adv*, 2014,4(8):087118.
 49. Goldey MB, Brawand NP, Vörös M, Galli G. Charge Transport in Nanostructured Materials: Implementation and Verification of Constrained Density Functional Theory. *J Chem Theory Comput*, 2017,13(6):2581–2590.
 50. Zarhri Z, Avilés Cardos MÁ, Ziat Y, Hammi M, El Rhazouani O, Cruz Argüello JC, et al. Synthesis, structural and crystal size effect on the optical properties of sprayed TiO₂ thin films: Experiment and DFT TB-mbj. *J Alloys Compd*, 2020,819:153010.
 51. Azam S, Abbas Z, Bilal Q, Irfan M, Khan MA, Naqib SH, et al. Effect of Fe doping on optoelectronic properties of CdS nanostructure: Insights from DFT calculations. *Phys B Condens Matter*, 2020,583:412056.
 52. Gao M-RYR, Xu Y-FF, Jiang JZ, Yu S-HH, Winter M, Brodd RJ, et al. Nanostructured metal chalcogenides: synthesis, modification, and applications in energy conversion and storage devices. *Chem Soc Rev*, 2013,42(7):2986–3017.
 53. Medles M, Benramdane N, Bouzidi A, Ahraoui K, Miloua R, Desfeux R, et al. Raman and optical studies of spray pyrolysed Sb₂S₃ thin films Raman and Optical Studies of spray pyrolysed Sb₂S₃ thin films. *J Optoelectron Adv*

- Mater*, 2014,16(5–6):726–731.
54. Jeroh M, Okoli D. Optical and structural properties of amorphous antimony sulphide thin films: Effect of dip time. *Adv Appl Sci Res*, 2012,3(2):793–800.
 55. Chate PA, Sathe DJ, Lakde SD, Bhabad VD. A novel method for the deposition of polycrystalline Sb₂S₃ thin films. *J Mater Sci Mater Electron*, 2016,27(12):12599–12603.
 56. Mane RS, Sankapal BR, Lokhande CD. Non-aqueous chemical bath deposition of Sb₂S₃ thin films. *Thin Solid Films*, 1999,353(12):30–33.
 57. Avilez Garcia RG, Meza Avendaño CA, Pal M, Paraguay Delgado F, Mathews NR. Antimony sulfide (Sb₂S₃) thin films by pulse electrodeposition: Effect of thermal treatment on structural, optical and electrical properties. *Mater Sci Semicond Process*, 2016,44:91–100.
 58. Pérez-Martínez D, Gonzaga-Sánchez JD, De Bray-Sánchez F, Vázquez-García G, Escorcía-García J, Nair MTS, et al. Simple solar cells of 3.5% efficiency with antimony sulfide-selenide thin films. *Phys status solidi - Rapid Res Lett*, 2016,10(5):388–396.
 59. Maghraoui-Meherzi H, Ben Nasr T, Kamoun N, Dachraoui M. Physical properties of chemically deposited Sb₂S₃ thin films. *Comptes Rendus Chim*, 2011,14(5):471–475.
 60. Lakhdar MH, Ouni B, Amlouk M. Thickness effect on the structural and optical constants of stibnite thin films prepared by sulfidation annealing of antimony films. *Optik (Stuttg)*, 2014,125(10):2295–2301.
 61. Wu W, Shan B, Feng K, Nan H. Resistive switching behavior of Sb₂S₃ thin film prepared by chemical bath deposition. *Mater Sci Semicond Process*, 2016,44:18–22.
 62. Kondrotas R, Chen C, Tang J. Sb₂S₃ Solar Cells. *Joule*, 2018,2(5):857–878.
 63. Ye Q, Xu Y, Chen W, Yang S, Zhu J, Weng J. Enhanced photovoltaic performance of Sb₂S₃-sensitized solar cells through surface treatments. *Appl Surf Sci*, 2018,440(May 15):294–299.
 64. Maiti N, Im SH, Lim C-S, Seok S II. A chemical precursor for depositing Sb₂S₃ onto mesoporous TiO₂ layers in nonaqueous media and its application to solar cells. *Dalt Trans*, 2012,41(38):11569.
 65. Itzhaik Y, Niitsoo O, Page M, Hodes G. Sb₂S₃-sensitized nanoporous TiO₂ solar cells. *J Phys Chem C*, 2009,113(11):4254–4256.

66. Varghese J, Barth S, Keeney L, Whatmore RW, Holmes JD. Nanoscale ferroelectric and piezoelectric properties of Sb₂S₃ nanowire arrays. *Nano Lett*, 2012,12(2):868–72.
67. Malakooti R, Cademartiri L, Migliori A, Ozin G a. Ultrathin Sb₂S₃ nanowires and nanoplatelets. *J Mater Chem*, 2008,18(1):66–69.
68. Hu H, Mo M, Yang B, Zhang X, Li Q, Yu W, et al. Solvothermal synthesis of Sb₂S₃ nanowires on a large scale. *J Cryst Growth*, 2003,258(1–2):106–112.
69. Wu Y, Nie P, Dou H, Jiang J, Zhu Y, Zhang X. Graphene scrolls coated Sb₂S₃ nanowires as anodes for sodium and lithium ion batteries. *Nano-Structures & Nano-Objects*, 2018,15:197–204.
70. Wang G, Cheung CL. Building crystalline Sb₂S₃ nanowire dandelions with multiple crystal splitting motif. *Mater Lett*, 2012,67(1):222–225.
71. Zhang H, Hu C, Ding Y, Lin Y. Synthesis of 1D Sb₂S₃ nanostructures and its application in visible-light-driven photodegradation for MO. *J Alloys Compd*, 2015,625:90–94.
72. Validžić ILLJ, Mitrić M, Abazović ND, Jokić BM, Milošević AS, Popović ZS, et al. Structural analysis, electronic and optical properties of the synthesized Sb₂S₃ nanowires with small band gap. *Semicond Sci Technol*, 2014,29(3):035007.
73. Pal M, Mathews NR, Mathew X. Surfactant-mediated self-assembly of Sb₂S₃ nanorods during hydrothermal synthesis. *J Mater Res*, 2017,32(03):530–538.
74. Zhang H, Ge M, Yang L, Zhou Z, Chen W, Li Q, et al. Synthesis and Catalytic Properties of Sb₂S₃ Nanowire Bundles as Counter Electrodes for Dye-Sensitized Solar Cells. *J Phys Chem C*, 2013,117(20):10285–10290.
75. Tellier C, Tossier A. *Size effects in thin films*. Elsevier, 2016.
76. Nozik AJ. Nanoscience and nanostructures for photovoltaics and solar fuels. *Nano Lett*, 2010,10(8):2735–2741.
77. Cohen ML, Chelikowsky JR. *Electronic Structure and Optical Properties of Semiconductors*. Springer Science & Business Media, 2012.
78. Ben Nasr T, Maghraoui-Meherzi H, Kamoun-Turki N. First-principles study of electronic, thermoelectric and thermal properties of Sb₂S₃. *J Alloys Compd*, 2016,663(5 April):123–127.
79. Chen J hua, Long X hao, Zhao C hua, Kang D, Guo J. DFT calculation on relaxation and electronic structure of sulfide minerals surfaces in presence of

- H₂O molecule. *J Cent South Univ*, 2014,21(10):3945–3954.
80. Koc H, Mamedov AM, Deligoz E, Ozisik H. First principles prediction of the elastic, electronic, and optical properties of Sb₂S₃ and Sb₂Se₃ compounds. *Solid State Sci*, 2012,14(8):1211–1220.
 81. Ben Nasr T, Maghraoui-Meherzi H, Ben Abdallah H, Bennaceur R. Electronic structure and optical properties of Sb₂S₃ crystal. *Phys B Condens Matter*, 2011,406(2):287–292.
 82. Filip MR, Patrick CE, Giustino F. GW quasiparticle band structures of stibnite, antimonselite, bismuthinite, and guanajuatite. *Phys Rev B - Condens Matter Mater Phys*, 2013,87(20):205125.
 83. Ibáñez J, Sans JA, Popescu C, López-Vidrier J, Elvira-Betanzos JJ, Cuenca-Gotor VP, et al. Structural, Vibrational, and Electronic Study of Sb₂S₃ at High Pressure. *J Phys Chem C*, 2016,120(19):10547–10558.
 84. Carey JJ, Allen JP, Scanlon DO, Watson GW. The electronic structure of the antimony chalcogenide series: Prospects for optoelectronic applications. *J Solid State Chem*, 2014,213:116–125.
 85. Liu Y, Ting K, Chua E, Chien T, Cde S, Gan CK. First-principles study of the lattice dynamics of Sb₂S₃. *Phys Chem Chem Phys*, 2014,16(1):345–350.
 86. Caruso F, Filip MR, Giustino F. Excitons in one-dimensional van der Waals materials: Sb₂S₃ nanoribbons. *Phys Rev B*, 2015,92(12):125134.
 87. Caracas R, Gonze X. First-principles study of the electronic properties of A₂B₃ minerals, with A=Bi,Sb and B=S,Se. *Phys Chem Miner*, 2005,32(4):295–300.
 88. Fabian J. Band structure and spin-orbit coupling engineering in transition-metal dichalcogenides. *Ann Phys*, 2014,526(9–10):A89–A91.
 89. Mane RS, Lokhande CD. Thickness-dependent properties of chemically deposited Sb₂S₃ thin films. *Mater Chem Phys*, 2003,82(2):347–354.
 90. Salem AM, Selim MS. Structure and optical properties of chemically deposited Sb₂S₃ thin films. *J Phys D Appl Phys*, 2001,34(1):12–17.
 91. Car R. Density functional theory: Fixing Jacob's ladder. *Nature Chemistry*. 2016,8(9):820–821.
 92. Zhang GX, Reilly AM, Tkatchenko A, Scheffler M. Performance of various density-functional approximations for cohesive properties of 64 bulk solids. *New J Phys*, 2018,20(6). doi:10.1088/1367-2630/aac7f0.

93. Weinmann D, Häusler W, Kramer B. Spin Blockades in Linear and Nonlinear Transport through Quantum Dots. *Phys Rev Lett*, 1995,74(6):984–987.
94. Sholl DS, Steckel JA. *Density Functional Theory: A Practical Introduction*. 2009.
95. Bertsch GF, Yabana K. Density Functional Theory. In: *Introduction to Modern Methods of Quantum Many-Body Theory and Their Applications*. World Scientific, 2006: 47–49.
96. Burke K. Perspective on density functional theory. *J Chem Phys*, 2012,136(15):150901.
97. Schwarz K. DFT calculations of solids with LAPW and WIEN2k. *J Solid State Chem*, 2003,176(2):319–328.
98. Blaha P, Madsen G. *WIEN2k*. 2010.
99. Blaha P, Schwarz K, Madsen G. *WIEN2K, An Augmented Plane Wave+ Local Orbitals Program for Calculating Crystal Properties*. 2001.
100. Cottenier S. *Density Functional Theory and the Family of (L)APW-methods: a step-by-step introduction*. 2013.
101. Otero de la Roza A, Luaña V. Runwien: a text-based interface for the WIEN package. *Comput Phys Commun*, 2009,180(5):800–812.
102. Iqbal M. Solar radiation Measuring instruments. In: *An Introduction to Solar Radiation*. Elsevier, 1983: 335–373.
103. Yang J. Potential applications of thermoelectric waste heat recovery in the automotive industry. *ICT 2005 24th Int Conf Thermoelectr 2005*, 2005,:155.
104. Einstein A. Über einen die Erzeugung und Verwandlung des Lichtes betreffenden heuristischen Gesichtspunkt. *Ann Phys*, 1905,322(6):132–148.
105. Purchase R, Vriend H, Groot H de, Harmsen P. *Artificial photosynthesis: for the conversion of sunlight to fuel*. Leiden University, 2015.
106. Würfel P. *Physics of solar cells : from basic principles to advanced concepts*. John Wiley & Sons, 2009.
107. Böer KW. The physics of solar cells. *J Appl Phys*, 1979,50(8):5356–5370.
108. Conibeer G. Third-generation photovoltaics. *Mater Today*, 2007,10(11):42–50.
109. Green M. *Third Generation Photovoltaics*. Springer: New York, 2003.
110. Delannoy Y. Purification of silicon for photovoltaic applications. *J Cryst Growth*, 2012,360(1):61–67.

111. Pizzini S. Towards solar grade silicon: Challenges and benefits for low cost photovoltaics. *Sol Energy Mater Sol Cells*, 2010,94(9):1528–1533.
112. Green MA. The path to 25% silicon solar cell efficiency: History of silicon cell evolution. *Prog Photovoltaics Res Appl*, 2009,17(3):183–189.
113. Chopra KL, Paulson PD, Dutta V. Thin-film solar cells: an overview. *Prog Photovoltaics Res Appl*, 2004,12(23):69–92.
114. Green MA. Thin-film solar cells: Review of materials, technologies and commercial status. *J Mater Sci Mater Electron*, 2007,18(1):15–19.
115. Re- N, May RM, Dooley JJ, Morgan MG, Reddy AKN, Williams RH, et al. Photovoltaic Technology : The Case for Thin-Film Solar Cells. *Science (80-)*, 2000,285(5428):692–699.
116. Green MA, Zhao J, Wang A, Wenham SR. Progress and outlook for high-efficiency crystalline silicon solar cells. *Sol Energy Mater Sol Cells*, 2001,65(1):9–16.
117. Nix WD. Mechanical properties of thin films. *Metall Trans A*, 1989,20(11):2217–2245.
118. Yalçın L, Öztürk R. Performance comparison of c-Si, mc-Si and a-Si thin film PV by PVsyst simulation. *J Optoelectron Adv Mater*, 2013,15(3–4):326–334.
119. Aberle AG. Thin-film solar cells. *Thin Solid Films*, 2009,517(17):4706–4710.
120. Lima FAS, Vasconcelos IF, Lira-Cantú M. Electrochemically synthesized mesoporous thin films of ZnO for highly efficient dye sensitized solar cells. *Ceram Int*, 2015,41(8):9314–9320.
121. Sankapal B, Tirpude A, Majumder S, Baviskar P. 1-D electron path of 3-D architecture consisting of dye loaded CdS nanowires: Dye sensitized solar cell. *J Alloys Compd*, 2015,651:399–404.
122. Green MA, Ho-Baillie A, Snaith HJ. The emergence of perovskite solar cells. *Nat Photonics*, 2014,8(7):506–514.
123. Asim N, Sopian K, Ahmadi S, Saeedfar K, Alghoul MA, Saadatian O, et al. A review on the role of materials science in solar cells. *Renew Sustain Energy Rev*, 2012,16(8):5834–5847.
124. Ramaswami R, Sivarajan KN, Sasaki GH (Galen H. *Optical networks : a practical perspective*. Elsevier/Morgan Kaufmann, 2010.
125. Goetzberger A, Luther J, Willeke G. Solar cells: Past, present, future. *Sol Energy Mater Sol Cells*, 2002,74(1–4):1–11.

126. Smestad G. Semiconductors for solar cells. *Sol Energy Mater Sol Cells*, 1996,43(4):425–426.
127. Xiang HJ, Huang B, Kan E, Wei SH, Gong XG. Towards direct-gap silicon phases by the inverse band structure design approach. *Phys Rev Lett*, 2013,110(11):118702.
128. Alharbi F, Bass JDJD, Salhi A, Alyamani A, Kim HCHC, Miller RDRD. Abundant non-toxic materials for thin film solar cells: Alternative to conventional materials. *Renew Energy*, 2011,36(10):2753–2758.
129. Taguchi M, Kawamoto K, Tsuge S, Baba T, Sakata H. HITTM cells—high-efficiency crystalline Si cells with novel structure. *Prog Photovoltaics Res Appl*, 2000,8(5):503.
130. Fortunato E, Ginley D, Hosono H, Paine DC. Transparent conducting oxides for photovoltaics. *MRS Bull*, 2007,32(3):242–247.
131. Noufi R, Zweibel K. High-efficiency CdTe and CIGS thin-film solar cells: Highlights and challenges. *Photovolt Energy Conversion, Conf Rec 2006 IEEE 4th World Conf 2006*, 2007,1:317–320.
132. Sönmezoğlu S, Termeli TA, Akin S, Askeroğlu I. Synthesis and characterization of tellurium-doped CdO nanoparticles thin films by sol-gel method. *J Sol-Gel Sci Technol*, 2013,67(1):97–104.
133. Al-Douri Y, Reshak AH, Baaziz H, Charifi Z, Khenata R, Ahmad S, et al. An ab initio study of the electronic structure and optical properties of CdS 1-x Te x alloys. *Sol Energy*, 2010,84(12):1979–1984.
134. Al-Douri Y, Baaziz H, Charifi Z, Khenata R, Hashim U, Al-Jassim M. Further optical properties of CdX (X=S, Te) compounds under quantum dot diameter effect: Ab initio method. *Renew Energy*, 2012,45:232–236.
135. Chandra A, Anderson G, Melkote S, Gao W, Haitjema H, Wegener K. Role of surfaces and interfaces in solar cell manufacturing. *CIRP Ann*, 2014,63(2):797–819.
136. Imamzai M, Aghaei M, Thayoob YH. A Review on Comparison between Traditional Silicon Solar Cells and Thin-Film CdTe Solar A Review on Comparison between Traditional Silicon Solar Cells and Thin- Film CdTe Solar Cells. In: *Proceedings National Graduate Conference 2012*. 2012: 1–5.
137. Fthenakis VM. Overview of Potential Hazards. In: *Practical Handbook of Photovoltaics*. Elsevier, 2012: 1083–1096.

138. Dumas E-M, Ozenne V, Mielke RE, Nadeau JL. Toxicity of CdTe quantum dots in bacterial strains. *IEEE Trans Nanobioscience*, 2009,8(1):58–64.
139. Cyrs WD, Avens HJ, Capshaw ZA, Kingsbury RA, Sahmel J, Tvermoes BE. Landfill waste and recycling: Use of a screening-level risk assessment tool for end-of-life cadmium telluride (CdTe) thin-film photovoltaic (PV) panels. *Energy Policy*, 2014,68:524–533.
140. Marwede M, Berger W, Schlummer M, Mäurer A, Reller A. Recycling paths for thin-film chalcogenide photovoltaic waste - Current feasible processes. *Renew Energy*, 2013,55:220–229.
141. Candelise C, Winskel M, Gross R. Implications for CdTe and CIGS technologies production costs of indium and tellurium scarcity. *Prog Photovoltaics Res Appl*, 2012,20(6):816–831.
142. Candelise C, Spiers JF, Gross RJK. Materials availability for thin film (TF) PV technologies development: A real concern? *Renew Sustain Energy Rev*, 2011,15(9):4972–4981.
143. Khan AD, Khan AD. Optimization of highly efficient GaAs–silicon hybrid solar cell. *Appl Phys A*, 2018,124(12):851.
144. Kodigala SR. *Introduction*. Elsevier Inc., 2010 doi:10.1016/B978-0-12-373697-0.00001-8.
145. Kumar YBK, Raja VS. Investigations on the growth of Cu₂ZnSnS₄ thin films for solar cell absorber layer. *Surfaces and Interfaces*, 2017,9:233–237.
146. Sinha S, Nandi DK, Kim SH, Heo J. Atomic-layer-deposited buffer layers for thin film solar cells using earth-abundant absorber materials: A review. *Sol Energy Mater Sol Cells*, 2018,176:49–68.
147. Todorov TK, Singh S, Bishop DM, Gunawan O, Lee YS, Gershon TS, et al. Ultrathin high band gap solar cells with improved efficiencies from the world's oldest photovoltaic material. *Nat Commun*, 2017,8(1):682.
148. Tumbul A, Aslan F, Göktaş A, Mutlu IH. All solution processed superstrate type Cu₂ZnSnS₄ (CZTS) thin film solar cell: Effect of absorber layer thickness. *J Alloys Compd*, 2019,781:280–288.
149. Belghachi A, Limam N. Effect of the absorber layer band-gap on CIGS solar cell. *Chinese J Phys*, 2017,55(4):1127–1134.
150. Berx M, Sarmadian N, Saniz R, Partoens B, Lamoen D. First-principles analysis of the spectroscopic limited maximum efficiency of photovoltaic

- absorber layers for CuAu-like chalcogenides and silicon. *Phys Chem Chem Phys*, 2016,18(30):20542–20549.
151. Shin MJ, Jo JH, Cho A, Gwak J, Yun JH, Kim K, et al. Semi-transparent photovoltaics using ultra-thin Cu(In,Ga)Se₂ absorber layers prepared by single-stage co-evaporation. *Sol Energy*, 2019,181:276–284.
 152. Banai RE, Horn MW, Brownson JRS. A review of tin (II) monosulfide and its potential as a photovoltaic absorber. *Solar Energy Materials and Solar Cells*. 2016,150:112–129.
 153. Gao F. *Advanced Nanomaterials for Solar Cells and Light Emitting Diodes*. Elsevier, 2019 doi:10.1016/c2017-0-00025-3.
 154. Yang JH, Yin WJ, Park JS, Ma J, Wei SH. Review on first-principles study of defect properties of CdTe as a solar cell absorber. *Semicond Sci Technol*, 2016,31(8):083002.
 155. Stuckelberger M, Biron R, Wyrsh N, Haug FJ, Ballif C. Review: Progress in solar cells from hydrogenated amorphous silicon. *Renew Sustain Energy Rev*, 2017,76:1497–1523.
 156. Ramanujam J, Singh UP. Copper indium gallium selenide based solar cells - A review. *Energy Environ Sci*, 2017,10(6):1306–1319.
 157. Welch AW, Baranowski LL, Peng H, Hempel H, Eichberger R, Unold T, et al. Trade-Offs in Thin Film Solar Cells with Layered Chalcostibite Photovoltaic Absorbers. *Adv Energy Mater*, 2017,7(11):1601935.
 158. Jamal MS, Bashar MS, Hasan AKM, Almutairi ZA, Alharbi HF, Alharthi NH, et al. Fabrication techniques and morphological analysis of perovskite absorber layer for high-efficiency perovskite solar cell: A review. *Renew Sustain Energy Rev*, 2018,98:469–488.
 159. Garcia-Llamas E, Merino JM, Gunder R, Neldner K, Greiner D, Steigert A, et al. Cu₂ZnSnS₄ thin film solar cells grown by fast thermal evaporation and thermal treatment. *Sol Energy*, 2017,141:236–241.
 160. Youn NK, Agawane GL, Nam D, Gwak J, Shin SW, Kim JH, et al. Cu₂ZnSnS₄ solar cells with a single spin-coated absorber layer prepared via a simple sol-gel route. *Int J Energy Res*, 2016,40(5):662–669.
 161. Shin D, Zhu T, Huang X, Gunawan O, Blum V, Mitzi DB. Brief review of emerging photovoltaic absorbers. *Adv Mater*, 2017,29(24):8–15.
 162. Shin D, Zhu T, Huang X, Gunawan O, Blum V, Mitzi DB. Chalcogenide

- Materials and Derivatives for Photovoltaic Applications. *Adv Mater*, 2017,29(24):1900819.
163. Shin D, Zhu T, Huang X, Gunawan O, Blum V, Mitzi DB. Annihilation of structural defects in chalcogenide absorber films for high-efficiency solar cells. *Adv Mater*, 2017,29(24):1818–1827.
 164. Shin D, Zhu T, Huang X, Gunawan O, Blum V, Mitzi DB. Earth-Abundant Chalcogenide Photovoltaic Devices with over 5% Efficiency Based on a Cu₂BaSn(S,Se)₄ Absorber. *Adv Mater*, 2017,29(24):1606945.
 165. Shin D, Zhu T, Huang X, Gunawan O, Blum V, Mitzi DB. Perovskite Chalcogenides with Optimal Bandgap and Desired Optical Absorption for Photovoltaic Devices. *Adv Mater*, 2017,29(24):1700216.
 166. Champness CH. Chalcogenide Photovoltaic Solar-Cells of Special Interest. *Phosphorus Sulfur Silicon Relat Elem*, 1988,38(3–4):385–397.
 167. Jensen WB. A note on the term "chalcogen". *J Chem Educ*, 1997,74(9):1063.
 168. Wang X, Tang R, Wu C, Zhu C, Chen T. Development of antimony sulfide–selenide Sb₂(S, Se)₃-based solar cells. *J Energy Chem*, 2018,27(3):713–721.
 169. Choi YC, Lee DU, Noh JH, Kim EK, Seok S Il. Highly improved Sb₂S₃ sensitized-inorganic-organic heterojunction solar cells and quantification of traps by deep-level transient spectroscopy. *Adv Funct Mater*, 2014,24(23):3587–3592.
 170. Kim D-H, Lee S-J, Park MS, Kang J-K, Heo JH, Im SH, et al. Highly reproducible planar Sb₂S₃ -sensitized solar cells based on atomic layer deposition. *Nanoscale*, 2014,6(23):14549–14554.
 171. Chen X, Li Z, Zhu H, Wang Y, Liang B, Chen J, et al. CdS/Sb₂S₃ heterojunction thin film solar cells with a thermally evaporated absorber. *J Mater Chem C*, 2017,5(36):9421–9428.
 172. Kyono A, Kimata M, Matsuhisa M, Miyashita Y, Okamoto K. Low-temperature crystal structures of stibnite implying orbital overlap of Sb_{5s}² inert pair electrons. *Phys Chem Miner*, 2002,29(4):254–260.
 173. Bayliss P, Nowacki W. Refinement of the crystal structure of stibnite, Sb₂S₃. *Zeitschrift für Krist Mater*, 1972,135(1–6):308–315.
 174. Šćavničar S. The crystal structure of stibnite A redetermination of atomic positions. *Zeitschrift für Krist*, 1960,114(1–6):85–97.
 175. Madelung O, Rössler U, Schulz M. *Non-Tetrahedrally Bonded Elements and*

- Binary Compounds I*. Springer-Verlag, 1998.
176. Kyono A, Kimata M. Structural variations induced by difference of the inert pair effect in the stibnite-bismuthinite solid solution series (Sb,Bi)₂S₃. *Am Mineral*, 2004,89(7):932–940.
 177. Khokhar AZ, De La Rue RM, Treble BM, McComb DW, Johnson NP. Stibnite inverse opal. *Micro Nano Lett*, 2008,3(1):1.
 178. Ghosh C, Varma BP. Optical properties of amorphous and crystalline Sb₂S₃ thin films. *Thin Solid Films*, 1979,60(1):61–65.
 179. Gonze X, Beuken JM, Caracas R, Detraux F, Fuchs M, Rignanese GM, et al. First-principles computation of material properties: the {ABINIT} software project. *Comput Mater Sci*, 2002,25(3):478.
 180. Shutov SD, Sobolev V V., Popov Y V., Shestatskii SN. Polarization Effects in the Reflectivity Spectra of Orthorhombic Crystals Sb₂S₃ and Sb₂Se₃. *Phys status solidi*, 1969,31(1):K23–K27.
 181. Hedin L. New Method for Calculating the One-Particle Green's Function with Application to the Electron-Gas Problem. *Phys Rev*, 1965,139(3A):A796–A823.
 182. El Mandouh ZS, Salama SN. Some physical properties of evaporated thin films of antimony trisulphide. *J Mater Sci*, 1990,25(3):1715–1718.
 183. El Zawawi I., Abdel-Moez A, Terra F, Mounir M. Substrate temperature effect on the optical and electrical properties of antimony trisulfide thin films. *Thin Solid Films*, 1998,324(1–2):300–304.
 184. Salem AM, Selim MS, Salem AM. Structure and optical properties of chemically deposited Sb₂S₃ thin films. *J Phys D Appl Phys*, 2001,34(1):12–17.
 185. Desai JD, Lokhande CD. Alkaline bath chemical deposition of antimony (III) sulphide thin films. *Thin Solid Films*, 1994,237(1–2):29–31.
 186. Chen H, Zhu C, Gan F. Preparation and Optical Properties of Sb₂S₃ Microcrystallite Doped Silica Glasses by the Sol-Gel Process. *J Sol-Gel Sci Technol*, 1998,12(1):181–184.
 187. Savadogo O, Mandal KC. Low-cost technique for preparing n-Sb₂S₃/p-Si heterojunction solar cells. *Appl Phys Lett*, 1993,63(2):228.
 188. Savadogo O, Mandal KC. Low Cost Schottky Barrier Solar Cells Fabricated on CdSe and Sb₂S₃ Films Chemically Deposited with Silicotungstic Acid. *J*

- Electrochem Soc*, 1994,141(10):2871.
189. Messina S, Nair MTS, Nair PK. Solar cells with Sb₂S₃ absorber films. *Thin Solid Films*, 2009,517(7):2503–2507.
 190. Muto T, Larramona G, Dennler G. Unexpected Performances of Flat Sb₂S₃-Based Hybrid Extremely Thin Absorber Solar Cells. *Appl Phys Express*, 2013,6(7):072301.
 191. Choi YC, Seok S II. Efficient Sb₂S₃-sensitized solar cells via single-step deposition of Sb₂S₃ using S/Sb-ratio-controlled SbCl₃-thiourea complex solution. *Adv Funct Mater*, 2015,25(19):2892–2898.
 192. Hagfeldt A, Boschloo G, Sun L, Kloo L, Pettersson H. Dye-sensitized solar cells. *Chem Rev*, 2010,110(11):6595–6663.
 193. Li X, Bai J, Zhou B, Yuan X, Zhang X, Liu L. High Performance of 3D Symmetric Flowerlike Sb₂S₃ Nanostructures in Dye-Sensitized Solar Cells. *Chem – A Eur J*, 2018,24(44):11444–11450.
 194. Lévy-Clément C, Tena-Zaera R, Ryan MA, Katty A, Hodes G. CdSe-Sensitized p-CuSCN/Nanowire n-ZnO Heterojunctions. *Adv Mater*, 2005,17(12):1512–1515.
 195. Oja I, Belaidi A, Dloczik L, Lux-Steiner M-C, Dittrich T. Photoelectrical properties of In(OH)_xS_y/PbS(O) structures deposited by SILAR on TiO₂. *Semicond Sci Technol*, 2006,21(4):520–526.
 196. Larramona G, Choné, C, Jacob A, Sakakura D, Delatouche B, Péré, D, et al. Nanostructured Photovoltaic Cell of the Type Titanium Dioxide, Cadmium Sulfide Thin Coating, and Copper Thiocyanate Showing High Quantum Efficiency. *Chem Mater*, 2006,18(6):1688–1696.
 197. Belaidi A, Dittrich T, Kieven D, Tornow J, Schwarzburg K, Lux-Steiner M. Influence of the local absorber layer thickness on the performance of ZnO nanorod solar cells. *Phys status solidi - Rapid Res Lett*, 2008,2(4):172–174.
 198. Page M, Niiitsoo O, Itzhaik Y, Cahen D, Hodes G. Copper sulfide as a light absorber in wet-chemical synthesized extremely thin absorber (ETA) solar cells. *Energy Environ Sci*, 2009,2(2):220–223.
 199. Shen F, Que W, He Y, Yuan Y, Yin X, Wang G. Enhanced Photocatalytic Activity of ZnO Microspheres via Hybridization with CuInSe₂ and CuInS₂ Nanocrystals. *ACS Appl Mater Interfaces*, 2012,4(8):4087–4092.
 200. Lan G-Y, Yang Z, Lin Y-W, Lin Z-H, Liao H-Y, Chang H-T. A simple

- strategy for improving the energy conversion of multilayered CdTe quantum dot-sensitized solar cells. *J Mater Chem*, 2009,19(16):2349.
201. Messina S, Nair MTS, Nair PK. Antimony sulphide thin film as an absorber in chemically deposited solar cells. *J Phys D Appl Phys*, 2008,41(9):095112.
 202. Versavel MY, Haber JA. Structural and optical properties of amorphous and crystalline antimony sulfide thin-films. *Thin Solid Films*, 2007,515(18):7171–7176.
 203. Parize R, Katerski A, Gromyko I, Rapenne L, Roussel H, Kärber E, et al. ZnO/TiO₂/Sb₂S₃ Core–Shell Nanowire Heterostructure for Extremely Thin Absorber Solar Cells. *J Phys Chem C*, 2017,121(18):9672–9680.
 204. Taretto K, Rau U. Modeling extremely thin absorber solar cells for optimized design. *Prog Photovoltaics Res Appl*, 2004,12(8):573–591.
 205. Ernst K, Belaidi A, K nenkamp R. Solar cell with extremely thin absorber on highly structured substrate. *Semicond Sci Technol*, 2003,18(6):475–479.
 206. Briscoe J, Dunn S. Extremely thin absorber solar cells based on nanostructured semiconductors. *Mater Sci Technol*, 2011,27(12):1741–1756.
 207. Yablonovitch E, Cody GD. Intensity enhancement in textured optical sheets for solar cells. *IEEE Trans Electron Devices*, 1982,29(2):300–305.
 208. Deckman HW, Wronski CR, Witzke H, Yablonovitch E. Optically enhanced amorphous silicon solar cells. *Appl Phys Lett*, 1983,42(11):968–970.
 209. Zheng Q, Wang C, Ma G, Jin M, Cheng S, Lai Y, et al. Annealing temperature impact on Sb₂S₃ solar cells prepared by spin-coating method. *Mater Lett*, 2019,243:104–107.
 210. Wedemeyer H, Michels J, Chmielowski R, Bourdais S, Muto T, Sugiura M, et al. Nanocrystalline solar cells with an antimony sulfide solid absorber by atomic layer deposition. *Energy Environ Sci*, 2013,6(1):67–71.
 211. Tsujimoto K, Nguyen D-C, Ito S, Nishino H, Matsuyoshi H, Konno A, et al. TiO₂ Surface Treatment Effects by Mg²⁺, Ba²⁺, and Al³⁺ on Sb₂S₃ Extremely Thin Absorber Solar Cells. *J Phys Chem C*, 2012,116(25):13465–13471.
 212. Huerta-Flores AM, García-Gómez NA, de la Parra-Arciniega SM, Sánchez EM. Fabrication and characterization of a nanostructured TiO₂/In₂S₃-Sb₂S₃/CuSCN extremely thin absorber (eta) solar cell. *Semicond Sci Technol*, 2016,31(8):085011.

213. Ito S, Tsujimoto K, Nguyen D-C, Manabe K, Nishino H. Doping effects in Sb₂S₃ absorber for full-inorganic printed solar cells with 5.7% conversion efficiency. *Int J Hydrogen Energy*, 2013,38(36):16749–16754.
214. Hodes G, Albu-Yaron A, Decker F, Motisuke P. Three-dimensional quantum-size effect in chemically deposited cadmium selenide films. *Phys Rev B*, 1987,36(8):4215–4221.
215. Takagahara T, Takeda K. Theory of the quantum confinement effect on excitons in quantum dots of indirect-gap materials. *Phys Rev B*, 1992,46(23):15578–15581.
216. Tran V, Soklaski R, Liang Y, Yang L. Layer-controlled band gap and anisotropic excitons in few-layer black phosphorus. *Phys Rev B*, 2014,89(23):235319.
217. Jing Y, Ma Y, Li Y, Heine T. GeP₃: A Small Indirect Band Gap 2D Crystal with High Carrier Mobility and Strong Interlayer Quantum Confinement. *Nano Lett*, 2017,17(3):1833–1838.
218. Kulkarni AN, Rajendra Prasad MB, Ingle R V., Pathan HM, Eldesoky GE, Naushad M, et al. Structural and optical properties of nanocrystalline Sb₂S₃ films deposited by chemical solution deposition. *Opt Mater (Amst)*, 2015,46:536–541.
219. Nair PK, Vázquez García G, Zamudio Medina EA, Guerrero Martínez L, Leyva Castrejón O, Moctezuma Ortiz J, et al. Antimony sulfide-selenide thin film solar cells produced from stibnite mineral. *Thin Solid Films*, 2018,645:305–311.
220. Wang Y, Herron N. Nanometer-sized semiconductor clusters: materials synthesis, quantum size effects, and photophysical properties. *J Phys Chem*, 1991,95(2):525–532.
221. Zimmermann E, Pfadler T, Kalb J, Dorman JA, Sommer D, Hahn G, et al. Toward High-Efficiency Solution-Processed Planar Heterojunction Sb₂S₃ Solar Cells. *Adv Sci*, 2015,2(5):1500059.
222. Srikanth S, Suriyanarayanan N, Prabahar S, Balasubramanian V, Kathirvel D. Structural and Optical Properties of Chemical bath Deposited Sb₂S₃ thin films. 2011,2(1):95–104.
223. Im J-H, Luo J, Franckevičius M, Pellet N, Gao P, Moehl T, et al. Nanowire Perovskite Solar Cell. *Nano Lett*, 2015,15(3):2120–2126.

224. Liu R, Wang J, Sun T, Wang M, Wu C, Zou H, et al. Silicon Nanowire/Polymer Hybrid Solar Cell-Supercapacitor: A Self-Charging Power Unit with a Total Efficiency of 10.5%. *Nano Lett*, 2017,17(7):4240–4247.
225. Tian B, Kempa TJ, Lieber CM. Single nanowire photovoltaics. *Chem Soc Rev*, 2009,38(1):16–24.
226. Zhang B-C, Wang H, He L, Duan C-Y, Li F, Ou X-M, et al. The diameter-dependent photoelectrochemical performance of silicon nanowires. *Chem Commun*, 2016,52(7):1369–1372.
227. Vietmeyer F, Chatterjee R, McDonald MP, Kuno M. Concerted single-nanowire absorption and emission spectroscopy: Explaining the origin of the size-dependent Stokes shift in single cadmium selenide nanowires. *Phys Rev B*, 2015,91(8):085422.
228. Luo S, Yu WB, He Y, Ouyang G. Size-dependent optical absorption modulation of Si/Ge and Ge/Si core/shell nanowires with different cross-sectional geometries. *Nanotechnology*, 2015,26(8):085702.
229. Han Q, Sun S, Sun D, Zhu J, Wang X. Room-temperature synthesis from molecular precursors and photocatalytic activities of ultralong Sb₂S₃ nanowires. *RSC Adv*, 2011,1(7):1364.
230. Geng ZR, Wang MX, Yue GH, Yan PX. Growth of single-crystal Sb₂S₃ nanowires via solvothermal route. *J Cryst Growth*, 2008,310(2):341–344.
231. Zhong M, Wang X, Liu S, Li B, Huang L, Cui Y, et al. High-performance photodetectors based on Sb₂S₃ nanowires: wavelength dependence and wide temperature range utilization. *Nanoscale*, 2017,9(34):12364–12371.
232. Cademartiri L, Ozin GA. Ultrathin Nanowires-A Materials Chemistry Perspective. *Adv Mater*, 2009,21(9):1013–1020.
233. Jensen IJT, Ulyashin AG, Løvvik OM. Direct-to-indirect bandgap transitions in ⟨110⟩ silicon nanowires. *J Appl Phys*, 2016,119(1):015702.
234. Senthil TSS, Muthukumarasamy N, Kang M. Study of various Sb₂S₃ nanostructures synthesized by simple solvothermal and hydrothermal methods. *Mater Charact*, 2014,95:164–170.
235. Huhn WP, Blum V. One-hundred-three compound band-structure benchmark of post-self-consistent spin-orbit coupling treatments in density functional theory. *Phys Rev Mater*, 2017,1(3):033803.
236. Gao W, Gao X, Abtey TA, Sun Y-Y, Zhang S, Zhang P. Quasiparticle band

- gap of organic-inorganic hybrid perovskites: Crystal structure, spin-orbit coupling, and self-energy effects. *Phys Rev B*, 2016,93(8):085202.
237. Fan X, Zheng W, Kuo J, Singh D, Sun C, reports WZ-S, et al. Modulation of electronic properties from stacking orders and spin-orbit coupling for 3R-type MoS₂. *nature.com*, <https://www.nature.com/articles/srep24140> (accessed 17 Feb 2019).
 238. Streltsov S V., Mazin II, Heid R, Bohnen K-P. Spin-orbit driven Peierls transition and possible exotic superconductivity in CsW₂O₆. *Phys Rev B*, 2016,94(24):241101.
 239. Kim H, Kang C-J, Kim K, Shim JH, Min BI. Suppression of the charge density wave instability in R₂O₂Bi(R= La, Er) due to large spin-orbit coupling. *Phys Rev B*, 2016,93(12):125116.
 240. Du Y, Bo X, Wang D, Kan E, Duan C-G, Savrasov SY, et al. Emergence of topological nodal lines and type-II Weyl nodes in the strong spin-orbit coupling system InNbX₂(X = S, Se). *Phys Rev B*, 2017,96(23):235152.
 241. Ren W, Wang A, Graf D, Liu Y, Zhang Z, Yin W-G, et al. Absence of Dirac states in BaZnBi₂ induced by spin-orbit coupling. *Phys Rev B*, 2018,97(3):035147.
 242. Streltsov S V., Cao G, Khomskii DI. Suppression of magnetism in Ba₅AlIr₂O₁₁ : Interplay of Hund's coupling, molecular orbitals, and spin-orbit interaction. *Phys Rev B*, 2017,96(1):014434.
 243. Rudenko AN, Katsnelson MI, Roldán R. Electronic properties of single-layer antimony: Tight-binding model, spin-orbit coupling, and the strength of effective Coulomb interactions. *Phys Rev B*, 2017,95(8):081407.
 244. Narsimha Rao E, Vaitheeswaran G, Reshak AH, Auluck S. Role of spin-orbit interaction on the nonlinear optical response of CsPbCO₃F using DFT. *Phys Chem Chem Phys*, 2017,19(46):31255–31266.
 245. Singh V, Pulikkotil JJ. Effects of spin-orbit coupling on the structural, electronic and magnetic properties of 3C-BaIrO₃. *Phys B Condens Matter*, 2017,519:59–62.
 246. Alluhaybi HA, Ghoshal SK, Alsobhi BO, Shamsuri WNNW. Electronic and optical correlation effects in bulk gold: Role of spin-orbit coupling. *Comput Condens Matter*, 2019,18:e00360.
 247. Makinistian L, Albanesi EA. First-principles calculations of the band gap and

- optical properties of germanium sulfide. *Phys Rev B*, 2006,74(4):045206.
248. Kim TY, Ferretti A, Park C-H. Effects of spin-orbit coupling on the optical response of a material. *Phys Rev B*, 2018,98(24):245410.
249. Jeong S-M, Yi S, Kim H-J, Bihlmayer G, Cho J-H. Competing edge structures of Sb and Bi bilayers generated by trivial and nontrivial band topologies. *Phys Rev B*, 2018,98(7):075402.
250. Zhuang HL, Cooper VR, Xu H, Ganesh P, Hennig RG, Kent PRC. Rashba effect in single-layer antimony telluroiodide SbTeI. *Phys Rev B*, 2015,92(11):115302.
251. Kealhofer R, Jang S, Griffin SM, John C, Benavides KA, Doyle S, et al. Observation of a two-dimensional Fermi surface and Dirac dispersion in YbMnSb 2. *Phys Rev B*, 2018,97(4):045109.
252. Hilal M, Rashid B, Khan SH, Khan A. Investigation of electro-optical properties of InSb under the influence of spin-orbit interaction at room temperature. *Mater Chem Phys*, 2016,184:41–48.
253. Guo SD. Importance of spin-orbit coupling in power factor calculations for half-Heusler ANiB (A = Ti, Hf, Sc, Y; B=Sn, Sb, Bi). *J Alloys Compd*, 2016,663:128–133.
254. Rahman MT, Haque E, Hossain MA. Elastic, electronic and thermoelectric properties of Sr3MN (M = Sb, Bi) under pressure. *J Alloys Compd*, 2019,783:593–600.
255. Xiong W, Xia C, Peng Y, Du J, Wang T, Zhang J, et al. Spin-orbit coupling effects on electronic structures in stanene nanoribbons. *Phys Chem Chem Phys*, 2016,18(9):6534–6540.
256. Franco de Carvalho F, Pignedoli CA, Tavernelli I. TDDFT-Based Spin–Orbit Couplings of 0D, 1D, and 2D Carbon Nanostructures: Static and Dynamical Effects. *J Phys Chem C*, 2017,121(18):10140–10152.
257. Nagarajan V, Chandiramouli R. Investigation of electronic properties and spin-orbit coupling effects on passivated stanene nanosheet: A first-principles study. *Superlattices Microstruct*, 2017,107:118–126.
258. Guo S-D, Wang J-L. Spin–orbital coupling effect on the power factor in semiconducting transition-metal dichalcogenide monolayers. *Semicond Sci Technol*, 2016,31(9):095011.
259. Wilhelm J, Walz M, Evers F. Ab initio spin-flip conductance of hydrogenated

- graphene nanoribbons: Spin-orbit interaction and scattering with local impurity spins. *Phys Rev B*, 2015,92(1).
260. Campos T, Faria Junior PE, Gmitra M, Sipahi GM, Fabian J. Spin-orbit coupling effects in zinc-blende InSb and wurtzite InAs nanowires: Realistic calculations with multiband $k \cdot p$ method. *Phys Rev B*, 2018,97(24):245402.
261. Magorrian SJ, Zólyomi V, Fal'ko VI. Spin-orbit coupling, optical transitions, and spin pumping in monolayer and few-layer InSe. *Phys Rev B*, 2017,96(19):195428.
262. Maier J. *Physical chemistry of ionic materials : ions and electrons in solids*. John Wiley, 2004.
263. Lee J. *Computational materials science: an introduction*. Crc Press, 2016.
264. Parrill A, Lipkowitz K. *Reviews in computational chemistry*. John Wiley & Sons, 2015.
265. William D Callister Jr. *Fundamentals of Materials Science and Engineering*. 2013.
266. Dirac PAM. Quantum mechanics of many-electron systems. *Proc R Soc Lond A*, 1929,123(792):714–733.
267. Ciccotti G, Ferrario M, Schuette C. *Molecular dynamics simulation*. 2014 <https://www.mdpi.com/books/pdfdownload/book/75/1> (accessed 29 Jan 2019).
268. Kumari I, Sandhu P, Ahmed M, Akhter Y. Molecular Dynamics Simulations, Challenges and Opportunities: A Biologist's Prospective. *Curr Protein Pept Sci*, 2017,18(11):1163–1179.
269. Hospital A, Goñi JR, Orozco M, Gelpí JL. Molecular dynamics simulations: advances and applications. *Adv Appl Bioinform Chem*, 2015,8:37–47.
270. Bernholc J. Computational Materials Science: The Era of Applied Quantum Mechanics. *Phys Today*, 1999,52(9):30–35.
271. Joseph L. . Baker J, Nicolas Biais N, Lorence Tama F, Michael J. . Bradley M, Enrique M. . De La Cruz E, Gregory A. . Voth G. Molecular dynamics simulations of large biomolecular complexes. *Curr Opin Struct Biol*, 2015,31:64–74.
272. Selvaraj C, Sakkiah S, Tong W, Hong H. Molecular dynamics simulations and applications in computational toxicology and nanotoxicology. *Food Chem Toxicol*, 2018,112:495–506.
273. Lundborg M, Wennberg C, Narangifard A, Lindahl E, Norlén L. Predicting

- drug permeability through skin using molecular dynamics simulation. *J Control Release*, 2018,283:269–279.
274. Huber RG, Marzinek JK, Holdbrook DA, Bond PJ. Multiscale molecular dynamics simulation approaches to the structure and dynamics of viruses. *Prog Biophys Mol Biol*, 2017,128:121–132.
275. Smirnov G, Stegailov VV. Efficiency of classical molecular dynamics algorithms on supercomputers. *Math Model Comput Simulations*, 2016,8(6). doi:10.1134/S2070048216060156.
276. Sanbonmatsu KY, Tung C-S. High performance computing in biology: multimillion atom simulations of nanoscale systems. *J Struct Biol*, 2007,157(3):470–80.
277. Tully JC. Molecular dynamics with electronic transitions. *J Chem Phys*, 1990,93(2):1061–1071.
278. Car R, Parrinello M. Unified Approach for Molecular Dynamics and Density-Functional Theory. *Phys Rev Lett*, 1985,55(22):2471–2474.
279. Saha SK, Ghosh P, Hens A, Murmu NC, Banerjee P. Density functional theory and molecular dynamics simulation study on corrosion inhibition performance of mild steel by mercapto-quinoline Schiff base corrosion inhibitor. *Phys E Low-Dimensional Syst Nanostructures*, 2015,66:332–341.
280. Leggett AJ. Reflections on the past, present and future of condensed matter physics. *Sci Bull*, 2018,63(16):1019–1022.
281. D’espagnat B. *Conceptual Foundations Of Quantum Mechanics*. CRC Press, 2018.
282. Lewars EG. *Computational Chemistry*. Springer Science & Business Media, 2011 doi:10.1007/978-90-481-3862-3.
283. Schrödinger E. Quantisierung als Eigenwertproblem. Dritte Mitteilung: Störungstheorie, mit Anwendung auf den Starkeffekt der Balmerlinien. *Ann Phys*, 1926,80(13):437–490.
284. Thiel W. Semiempirical quantum-chemical methods. *Wiley Interdiscip Rev Comput Mol Sci*, 2014,4(2):145–157.
285. Thiel W. Semiempirical methods: current status and perspectives. *Tetrahedron*, 1988,44(24):7393–7408.
286. Hartree DR. The Wave Mechanics of an Atom with a Non-Coulomb Central Field. Part I. Theory and Methods. *Math Proc Cambridge Philos Soc*,

- 1928,24(03):426.
287. Slater JC. Note on Hartree's Method. *Phys Rev*, 1930,35(2):210–211.
288. Fock V. Näherungsmethode zur Lösung des quantenmechanischen Mehrkörperproblems. *Zeitschrift für Phys*, 1930,61(1–2):126–148.
289. Qorbani M, Naseri N, Moshfegh AZ. Hierarchical Co₃O₄/Co(OH)₂ Nanoflakes as a Supercapacitor Electrode: Experimental and Semi-Empirical Model. *ACS Appl Mater Interfaces*, 2015,7(21):11172–11179.
290. T.M. N, K. K, J.A.J. M, A.J. H, D. van de M. A semi-empirical model for transport of inorganic nanoparticles across a lipid bilayer: Implications for uptake by living cells. *Environ Toxicol Chem*, 2015,34(3):488–496.
291. Gregor K, Shijing S, Anthony KC. Solid-state principles applied to organic–inorganic perovskites: new tricks for an old dog. *Chem Sci*, 2014,5:4712–4715.
292. Miriyala VM, Řezáč J. Testing Semiempirical Quantum Mechanical Methods on a Data Set of Interaction Energies Mapping Repulsive Contacts in Organic Molecules. *J Phys Chem A*, 2018,122(10):2801–2808.
293. Meng L, Zhang Y, Wan X, Li C, Zhang X, Wang Y, et al. SI_Organic and solution-processed tandem solar cells with 17.3% efficiency. *Science (80-)*, 2018,1098(September):eaat2612.
294. Christensen AS, Kubař T, Cui Q, Elstner M. Semiempirical Quantum Mechanical Methods for Noncovalent Interactions for Chemical and Biochemical Applications. *Chem Rev*, 2016,116(9):5301–37.
295. Hohenberg, P.; Kohn W. Hohenberg, P.; Kohn, W. *Phys Rev*, 1964,136(3B):B864–B871.
296. Kohn W, Sham LJ. Self-Consistent Equations Including Exchange and Correlation Effects. *Phys Rev*, 1965,140(4A):A1133–A1138.
297. Mardirossian N, Head-Gordon M. Thirty years of density functional theory in computational chemistry: an overview and extensive assessment of 200 density functionals. *Mol Phys*, 2017,115(19):2315–2372.
298. Jain A, Shin Y, Persson KA. Computational predictions of energy materials using density functional theory. *Nat Rev Mater*, 2016,1(1):15004.
299. Becke AD. Perspective: Fifty years of density-functional theory in chemical physics. *J Chem Phys*, 2014,140(18):18A301.
300. Butler KT, Frost JM, Skelton JM, Svane KL, Walsh A. Computational

- materials design of crystalline solids. *Chem Soc Rev*, 2016,45(22):6138–6146.
301. Oviedo OA, Leiva EPM. Computational study of nanostructured materials. *Curr Opin Electrochem*, 2017,1(1):1–6.
 302. Aliano A, Cicero G, Nili H, Green NG, García-Sánchez P, Ramos A, et al. Ab Initio DFT Simulations of Nanostructures. In: *Encyclopedia of Nanotechnology*. Springer Netherlands: Dordrecht, 2012: 11–17.
 303. Born M, Oppenheimer R. Zur Quantentheorie der Molekeln. *Ann Phys*, 1927,389(20):457–484.
 304. Amusia MY, Msezane a Z, Shaginyan VR. Density Functional Theory versus the Hartree Fock Method: Comparative Assessment. *ArXiv*, 2002,T68(0204104v2):16.
 305. March N. *Self-consistent fields in atoms: Hartree and Thomas–Fermi atoms*. Elsevier, 2016.
 306. Piela L. *Ideas of quantum chemistry*. Second Edi. Elsevier, 2014.
 307. Pauli W. Über den Zusammenhang des Abschlusses der Elektronengruppen im Atom mit der Komplexstruktur der Spektren. *Zeitschrift für Phys*, 1925,31(1):765–783.
 308. Gonis A. Generalization of the variational principle and the Hohenberg and Kohn theorems for excited states of Fermion systems. *Phys Lett A*, 2017,381(1):48–52.
 309. Slater JC. The Theory of Complex Spectra. *Phys Rev*, 1929,34(10):1293–1322.
 310. Fermi E. A statistical method for determining some properties of the atom. I. *Atti della Accad Naz dei Lincei, Cl di Sci Fis Mat e Nat Rend*, 1927,6:602–607.
 311. Fermi E. Eine statistische Methode zur Bestimmung einiger Eigenschaften des Atoms und ihre Anwendung auf die Theorie des periodischen Systems der Elemente. *Zeitschrift für Phys*, 1928,48(1–2):73–79.
 312. Hohenberg P, Kohn W, Rajagopal AK, Callaway J. Inhomogeneous electron gas. *Phys Rev*, 1964,7(3B):B864–B871.
 313. Langreth DC, Perdew JP. Theory of nonuniform electronic systems. I. Analysis of the gradient approximation and a generalization that works. *Phys Rev B*, 1980,21(12):5469–5493.
 314. Mohamad M, Ul Haq B, Ahmed R, Shaari A, Ali N, Hussain R. A density

- functional study of structural, electronic and optical properties of titanium dioxide: Characterization of rutile, anatase and brookite polymorphs. *Mater Sci Semicond Process*, 2015,31:405–414.
315. Menezla S, Kadri A, Zitouni K, Djelal A, Djermouni M, Hallouche A, et al. Ab-initio DFT FP-LAPW GGA and LDA TB-mBJ and SO theoretical study of structural and elastic properties of Zinc-Blende crystal phase GaAs_{1-x}Bix alloys. *Superlattices Microstruct*, 2015,88:18–31.
316. Biskri ZE, Rached H, Boucheur M, Rached D. Computational study of structural, elastic and electronic properties of lithium disilicate (Li₂Si₂O₅) glass-ceramic. *J Mech Behav Biomed Mater*, 2014,32:345–350.
317. Deringer VL, Stoffel RP, Wuttig M, Dronskowski R. Vibrational properties and bonding nature of Sb₂Se₃ and their implications for chalcogenide materials. *Chem Sci*, 2015,6(9):5255–5262.
318. Shang S, Wang Y, Guan P, Wang WY, Fang H, Anderson T, et al. Insight into structural, elastic, phonon, and thermodynamic properties of α -sulfur and energy-related sulfides: a comprehensive first-principles study. *J Mater Chem A*, 2015,3(15):8002–8014.
319. Parr RG, Yang W. Density-Functional Theory of the Electronic Structure of Molecules. *Annu Rev Phys Chem*, 1995,46(1):701–728.
320. Jiang H. First-principles approaches for strongly correlated materials: A theoretical chemistry perspective. *Int J Quantum Chem*, 2015,115(11):722–730.
321. Seminario JM, Politzer P. *Modern density functional theory : a tool for chemistry*. Elsevier, 1995.
322. Wu Z, Cohen RE. More accurate generalized gradient approximation for solids. *Phys Rev B - Condens Matter Mater Phys*, 2006,73(23):235116.
323. Perdew JJP, Burke K, Ernzerhof M. Generalized Gradient Approximation Made Simple. *Phys Rev Lett*, 1996,77(18):3865–3868.
324. Perdew JP, Ruzsinszky A, Csonka GI, Vydrov OA, Scuseria GE, Constantin LA, et al. Restoring the Density-Gradient Expansion for Exchange in Solids and Surfaces. *Phys Rev Lett*, 2008,100(13):136406.
325. Engel E, Vosko SH. Exact exchange-only potentials and the virial relation as microscopic criteria for generalized gradient approximations. *Phys Rev B*, 1993,47(20):13164–13174.

326. Maeda T, Wada T. First-principles study of electronic structure of CuSbS₂ and CuSbSe₂ photovoltaic semiconductors. *Thin Solid Films*, 2015,582:401–407.
327. Moussa R, Abdiche A, Khenata R, Wang XT, Varshney D, Sun XW, et al. Structural, electronic, optical, thermodynamic and elastic properties of the zinc-blende Al_xIn_{1-x}N ternary alloys: A first principles calculations. *J Phys Chem Solids*, 2018,119:36–49.
328. Wang B-T, Souvatzis P, Eriksson O, Zhang P. Lattice dynamics and chemical bonding in Sb₂Te₃ from first-principles calculations. *J Chem Phys*, 2015,142(17):174702.
329. Lawal A, Shaari A, Ahmed R, Jarkoni N. First-principles investigations of electron-hole inclusion effects on optoelectronic properties of Bi₂Te₃, a topological insulator for broadband photodetector. *Phys B Condens Matter*, 2017,520:69–75.
330. Kumagai Y, Burton LA, Walsh A, Oba F. Electronic Structure and Defect Physics of Tin Sulfides: SnS, Sn₂S₃, and SnS₂. *Phys Rev Appl*, 2016,6(1):014009.
331. Nguyen C V., Hieu NN, Nguyen DT. Dispersion-Corrected Density Functional Theory Investigations of Structural and Electronic Properties of Bulk MoS₂: Effect of Uniaxial Strain. *Nanoscale Res Lett*, 2015,10(1):433.
332. Bilal M, Ahmad I, Rahnamaye Aliabad HA, Jalali Asadabadi S. Detailed DFT studies of the band profiles and optical properties of antiperovskites SbN₃Ca₃ and BiN₃Ca₃. *Comput Mater Sci*, 2014,85:310–315.
333. Irshad Z, Shah SH, Rafiq MA, Hasan MM. First principles study of structural, electronic and magnetic properties of ferromagnetic Bi₂Fe₄O₉. *J Alloys Compd*, 2015,624:131–136.
334. Yuk SF, Pitike KC, Nakhmanson SM, Eisenbach M, Li YW, Cooper VR. Towards an accurate description of perovskite ferroelectrics: exchange and correlation effects. *Sci Rep*, 2017,7(1):43482.
335. Dufek P, Blaha P, Schwarz K. Applications of Engel and Voskos generalized gradient approximation in solids. *Phys Rev B*, 1994,50(11):7279–7283.
336. Kohanoff J, Gidopoulos N. Density functional theory: basics, new trends and applications. In: *Handbook of molecular physics and ...*. 2003: 532–568.
337. Drablia S, Boukhris N, Boulechfar R, Meradji H, Ghemid S, Ahmed R, et al.

- Ab initio calculations of the structural, electronic, thermodynamic and thermal properties of BaSe_{1-x}Te_x alloys. *Phys Scr*, 2017,92(10):105701.
338. Muhammad N, Khan A, Haidar Khan S, Sajjaj Siraj M, Shah SSA, Murtaza G. Engel-Vosko GGA calculations of the structural, electronic and optical properties of LiYO₂. *Phys B Condens Matter*, 2017,521:62–68.
339. Faizan M, Murtaza G, Khan SH, Khan A, Mehmood A, Khenata R, et al. First-principles study of the double perovskites Sr₂XOsO₆ (X = Li, Na, Ca) for spintronics applications. *Bull Mater Sci*, 2016,39(6):1419–1425.
340. Becke AD, Johnson ER. A simple effective potential for exchange. *J Chem Phys*, 2006,124(22):221101.
341. Tran F, Blaha P. Accurate Band Gaps of Semiconductors and Insulators with a Semilocal Exchange-Correlation Potential. *Phys Rev Lett*, 2009,102(22):226401.
342. Mondal S, Mazumdar C, Ranganathan R, Alleno E, Sreeparvathy PC, Kanchana V, et al. Ferromagnetically correlated clusters in semimetallic Ru₂NbAl Heusler alloy and its thermoelectric properties. *Phys Rev B*, 2018,98(20):205130.
343. Ul Haq B, AlFaify S, Ahmed R, Butt FK, Laref A, Shkir M. Exploring single-layered SnSe honeycomb polymorphs for optoelectronic and photovoltaic applications. *Phys Rev B*, 2018,97(7):075438.
344. Traoré B, Boudier G, Lafargue-Dit-Hauret W, Rocquefelte X, Katan C, Tran F, et al. Efficient and accurate calculation of band gaps of halide perovskites with the Tran-Blaha modified Becke-Johnson potential. *Phys Rev B*, 2019,99(3):035139.
345. Ye Z, Cui S, Shu T, Ma S, Liu Y, Sun Z, et al. Electronic band structure of epitaxial PbTe (111) thin films observed by angle-resolved photoemission spectroscopy. *Phys Rev B*, 2017,95(16):165203.
346. Shi H, Ming W, Du M-H. Bismuth chalcogenides and oxyhalides as optoelectronic materials. *Phys Rev B*, 2016,93(10):104108.
347. Ondračka P, Holec D, Nečas D, Kedroňová E, Elisabeth S, Goulet A, et al. Optical properties of Ti_xSi_{1-x}O₂ solid solutions. *Phys Rev B*, 2017,95(19):195163.
348. Li Y, Singh DJ. Properties of the ferroelectric visible light absorbing semiconductors: Sn₂P₂S₆ and Sn₂P₂Se₆. *Phys Rev Mater*, 2017,1(7):075402.

349. Jiang H. Band gaps from the Tran-Blaha modified Becke-Johnson approach: A systematic investigation. *J Chem Phys*, 2013,138(13):134115.
350. Singh DJ. Electronic structure calculations with the Tran-Blaha modified Becke-Johnson density functional. *Phys Rev B*, 2010,82(20):205102.
351. Dunning TH, Hay PJ. Gaussian Basis Sets for Molecular Calculations. In: *Methods of Electronic Structure Theory*. Springer US: Boston, MA, 1977: 1–27.
352. Slater JC. Wave Functions in a Periodic Potential. *Phys Rev*, 1937,51(10):846–851.
353. Bloch F. Über die quantenmechanik der elektronen in kristallgittern. *Zeitschrift für Phys*, 1929,52(7–8):555–600.
354. Blöchl PE, Jepsen O, Andersen OK. Improved tetrahedron method for Brillouin-zone integrations. *Phys Rev B*, 1994,49(23):16223–16233.
355. Monkhorst H, Pack J. Special points for Brillouin zone integrations. *Phys Rev B*, 1976,13(12):5188–5192.
356. Segall MD, Shah R, Pickard CJ, Payne MC. Population analysis of plane-wave electronic structure calculations of bulk materials. *Phys Rev B*, 1996,54(23):16317–16320.
357. Troullier N, Martins JL. Efficient pseudopotentials for plane-wave calculations. *Phys Rev B*, 1991,43(3):1993–2006.
358. Petersen M, Wagner F, Hufnagel L, Scheffler M, Blaha P, Schwarz K. Improving the efficiency of FP-LAPW calculations. *Comput Phys Commun*, 2000,126(3):294–309.
359. Andersen OK. Linear methods in band theory. *Phys Rev B*, 1975,12(8):3060–3083.
360. Takeda T, Kubler J. Linear augmented plane wave method for self-consistent calculations. *J Phys F Met Phys*, 1979,9(4):661.
361. Perdew JP, Wang Y. Pair-distribution function and its coupling-constant average for the spin-polarized electron gas. *Phys Rev B*, 1992,46(20):12947–12954.
362. Leszczynski J, Shukla MK. *Practical Aspects of Computational Chemistry*. Springer: New York, 2009.
363. Singh D. *Plane waves, pseudopotential and the LAPW method*. Boston, *Dortrecht*. Dortrecht, 1994.

364. Martins RM. *Electronic Structure: Basic Theory And Practical Methods*. Cambridge university press, 2004 doi:10.1080/00107514.2010.509989.
365. Schlegel HB. Geometry optimization. *Wiley Interdiscip Rev Comput Mol Sci*, 2011,1(5):790–809.
366. Birch F. Finite elastic strain of cubic crystals. *Phys Rev*, 1947,71(11):809–824.
367. Ahmed SN. *Physics and Engineering of Radiation Detection*. Academic Press, 2007.
368. Kittel C. Introduction to solid state physics. *Solid State Phys*, 2005,:703.
369. Kakani, S. L, Bhandari, K. C. *Electronics Theory and Applications*. New Age International, 2011.
370. Yuan L-D, Deng H-X, Li S-S, Wei S-H, Luo J-W. Unified theory of direct or indirect band-gap nature of conventional semiconductors. *Phys Rev B*, 2018,98(24):245203.
371. Dirac PAM. On the Theory of Quantum Mechanics. *Proc R Soc A Math Phys Eng Sci*, 1926,112(762):661–677.
372. Fermi E. Sulla quantizzazione del gas perfetto monoatomico. *Rend Lincei*, 1926,3:145–149.
373. Perdew JP. Density functional theory and the band gap problem. *Int J Quantum Chem*, 1985,28(19 S):497–523.
374. Seidl A, Görling A, Vogl P, Majewski J, Levy M. Generalized Kohn-Sham schemes and the band-gap problem. *Phys Rev B - Condens Matter Mater Phys*, 1996,53(7):3764–3774.
375. Kao K. *Dielectric phenomena in solids*. Elsevier, 2004.
376. Prasad R. *Electronic structure of materials*. Crc Press, 2013.
377. Perdew JP. Climbing the ladder of density functional approximations. *MRS Bull*, 2013,38(9):743–750.
378. Bohm D, Pines D. A Collective Description of Electron Interactions. I. Magnetic Interactions. *Phys Rev*, 1951,82(5):625–634.
379. Pines D, Bohm D. A Collective Description of Electron Interactions: II. Collective vs Individual Particle Aspects of the Interactions. *Phys Rev*, 1952,85(2):338–353.
380. Bohm D, Pines D. A Collective Description of Electron Interactions: III. Coulomb Interactions in a Degenerate Electron Gas. *Phys Rev*, 1953,92(3):609–625.

381. Eshuis H, Bates JE, Furche F. Electron correlation methods based on the random phase approximation. *Theor Chem Acc*, 2012,131(1):1084.
382. Miyake T, Aryasetiawan F, Kotani T, van Schilfgaarde M, Usuda M, Terakura K. Total energy of solids: An exchange and random-phase approximation correlation study. *Phys Rev B*, 2002,66(24):245103.
383. Ren X, Rinke P, Joas C, Scheffler M. Random-phase approximation and its applications in computational chemistry and materials science. *J Mater Sci*, 2012,47(21):7447–7471.
384. Olsen T, Thygesen KS. Random phase approximation applied to solids, molecules, and graphene-metal interfaces: From van der Waals to covalent bonding. *Phys Rev B*, 2013,87(7):075111.
385. Gavrilenko VI, Bechstedt F. Optical functions of semiconductors beyond density-functional theory and random-phase approximation. *Phys Rev B*, 1997,55(7):4343–4352.
386. Ul B, Ahmed R, Yull J, Shaari A, Alfaify S, Ahmed M. Composition-induced influence on the electronic band structure, optical and thermoelectric coefficients of the highly mismatched GaNSb alloy over the entire range: A DFT analysis. *J Alloys Compd*, 2017,693:1020–1027.
387. Ataei SS, Mohammadzadeh MR, Seriani N. Excitonic effects in the optical properties of hydrogenated anatase TiO₂. *Phys Rev B*, 2017,95(15):155205.
388. Ehrenreich H, Cohen MH. Self-Consistent Field Approach to the Many-Electron Problem. *Phys Rev*, 1959,115(4):786–790.
389. Gajdoš M, Hummer K, Kresse G, Furthmüller J, Bechstedt F. Linear optical properties in the projector-augmented wave methodology. *Phys Rev B*, 2006,73(4):045112.
390. Kramers HA. La diffusion de la lumière par les atomes. *Atti cong intern Fis (Transactions Volta Centen Congr*, 1927,2:545.
391. de L. Kronig R. On the Theory of Dispersion of X-Rays. *J Opt Soc Am*, 1926,12(6):547.
392. Lucarini V, Saarinen J, Peiponen K, Vartiainen E. *Kramers-Kronig Relations in Optical Materials Research*. Springer Science & Business Media, 2005.
393. Schwarz K, Blaha P, Trickey SBB. Electronic structure of solids with WIEN2k. *Mol Phys*, 2010,108(21–23):3147–3166.
394. Parr RG, Yang W. T. *Density-Functional Theory of Atoms and Molecules*.

- Oxford University Press, 1989.
395. Chadi DJ. Special points for Brillouin-zone integrations. *Phys Rev B*, 1977,16(4):1746–1747.
 396. Schwarz, K.Blaho P, Madsen GKHKH. Electronic structure calculations of solids using the WIEN2k package for material sciences. *Comput Phys Commun*, 2002,147(1–2):71–76.
 397. Assali A, Bouzlama M, Chaabane L, Mokadem A, Saidi F. Structural and opto-electronic properties of InP1–xBixbismide alloys for MID–infrared optical devices: A DFT + TB-mBJ study. *Phys B Condens Matter*, 2017,526:71–79.
 398. Usman T, Murtaza G, Luo H, Mahmood A. GGA and GGA + U Study of Rare Earth-Based Perovskites in Cubic Phase. *J Supercond Nov Magn*, 2017,30(6):1389–1396.
 399. Fischer M, Evers FO, Formalik F, Olejniczak A. Benchmarking DFT-GGA calculations for the structure optimisation of neutral-framework zeotypes. *Theor Chem Acc*, 2016,135(12). doi:10.1007/s00214-016-2014-6.
 400. Quertinmont J, Carletta A, Tumanov NA, Leyssens T, Wouters J, Champagne B. Assessing density functional theory approaches for predicting the structure and relative energy of salicylideneaniline molecular switches in the solid state. *J Phys Chem C*, 2017,121(12):6898–6908.
 401. Ali IOA, Joubert DP, Suleiman MSH. A theoretical investigation of structural, mechanical, electronic and thermoelectric properties of orthorhombic CH₃NH₃PbI₃. *Eur Phys J B* 2018 9110, 2018,91(10):1–8.
 402. Hoat DM. Theoretical investigations on physical properties of SrFCuCh (Ch=S and Se). *J Solid State Chem*, 2019,271:191–198.
 403. Siddique M, Rahman AU, Iqbal A, Haq BU, Azam S, Nadeem A, et al. A Systematic First-Principles Investigation of Structural, Electronic, Magnetic, and Thermoelectric Properties of Thorium Monopnictides ThPn (Pn = N, P, As): A Comparative Analysis of Theoretical Predictions of LDA, PBEsol, PBE-GGA, WC-GGA, and LDA + U Me. *Int J Thermophys*, 2019,40(12). doi:10.1007/s10765-019-2572-7.
 404. Mahanty S, Merino JM, León M. Preparation and optical studies on flash evaporated Sb₂S₃ thin films. *J Vac Sci Technol A Vacuum, Surfaces, Film*, 1998,15(6):3060.

405. Black J, Conwell EM, Seigle L, Spencer CW. Electrical and optical properties of some M_2V-bN_3VI-b semiconductors. *J Phys Chem Solids*, 1957,2(3):240–251.
406. Bube RH. Photoelectronic Analysis of High Resistivity Crystals: (a) GaAs, (b) Sb_2S_3 . *J Appl Phys*, 1960,31(2):315–322.
407. Yesugade NS, Lokhande CD, Bhosale CH. Structural and optical properties of electrodeposited Bi_2S_3 , Sb_2S_3 and As_2S_3 thin films. *Thin Solid Films*, 1995,263(2):145–149.
408. Patrick CE, Giustino F. Structural and Electronic Properties of Semiconductor-Sensitized Solar-Cell Interfaces. *Adv Funct Mater*, 2011,21(24):4663–4667.
409. Vadapoo R, Krishnan S, Yilmaz H, Marin C. Self-standing nanoribbons of antimony selenide and antimony sulfide with well-defined size and band gap. *Nanotechnology*, 2011,22(17):175705.
410. Wang X, Tang R, Wu C, Zhu C, Chen T. Development of antimony sulfide-selenide $Sb_2(S, Se)_3$ -based solar cells. *J Energy Chem*, 2018,27(3):713–721.
411. Pourghazi A, Dadsetani M. Electronic and optical properties of BaTe, BaSe and BaS from first principles. *Phys B Condens Matter*, 2005,370(1–4):35–45.
412. Huhn WP, Blum V. One-hundred-three compound band-structure benchmark of post-self-consistent spin-orbit coupling treatments in density functional theory. *Phys Rev Mater*, 2017,1(3):033803.
413. Lawal A, Shaari A, Ahmed R, Jarkoni N. First-principles many-body comparative study of Bi_2Se_3 crystal: A promising candidate for broadband photodetector. *Phys Lett A*, 2017,381(35):2993–2999.
414. Lawal A, Shaari A, Ahmed R, Jarkoni N. Sb_2Te_3 crystal a potential absorber material for broadband photodetector: A first-principles study. *Results Phys*, 2017,7:2302–2310.
415. Demján T, Vörös M, Palummo M, Gali A. Electronic and optical properties of pure and modified diamondoids studied by many-body perturbation theory and time-dependent density functional theory. *J Chem Phys*, 2014,141(6):064308.
416. Haus JW, de Ceglia D, Vincenti MA. Plasmonics. In: *Fundamentals and Applications of Nanophotonics*. Woodhead Publishing, 2016: 233–252.
417. Sharma Y, Srivastava P, Dashora A, Vadkhiya L, Bhayani MK, Jain R, et al. Electronic structure, optical properties and Compton profiles of Bi_2S_3 and

- Bi₂Se₃. *Solid State Sci*, 2012,14(2):241–249.
418. Koc H, Ozisik H, Deligöz E, Mamedov AM, Ozbay E. Mechanical, electronic, and optical properties of Bi₂S₃ and Bi₂Se₃ compounds: first principle investigations. *J Mol Model*, 2014,20(4):2180.
419. Lavrentyev AA, Gabrelian B V., Vu VT, Shkumat PN, Ocheretova VA, Parasyuk O V., et al. Electronic structure and optical properties of Cu₂CdGeS₄: DFT calculations and X-ray spectroscopy measurements. *Opt Mater (Amst)*, 2015,47:435–444.
420. Schubert M, Hofmann T, Herzinger CM, Dollase W. Generalized ellipsometry for orthorhombic, absorbing materials: dielectric functions, phonon modes and band-to-band transitions of Sb₂S₃. *Thin Solid Films*, 2004,455:619–623.
421. Penn DR. Wave-Number-Dependent Dielectric Function of Semiconductors. *Phys Rev*, 1962,128(5):2093–2097.
422. Hall JA. Uniform Layer Hetero-Junction Targets for Television Camera Tubes. *Adv Electron Electron Phys*, 1972,33:229–240.
423. Țigău N, Gheorghieș C, Rusu GI, Condurache-Bota S. The influence of the post-deposition treatment on some physical properties of Sb₂S₃ thin films. *J Non Cryst Solids*, 2005,351(12–13):987–992.
424. Sakr GB, Yahia IS, El-Komy GM, Salem AM. Optical properties of thermally evaporated Bi₂Se₃ thin films treated with AgNO₃ solution. *Surf Coatings Technol*, 2011,205(12):3553–3558.
425. Fox M, Bertsch GF. *Optical Properties of Solids*. *Am J Phys*, 2002,70(12):1269–1270.
426. Wypych G. *Handbook of fillers*. Elsevier, 2000.
427. Chakrabarti A, Hermann K, Druzinic R, Witko M, Wagner F, Petersen M. Geometric and electronic structure of vanadium pentoxide: A density functional bulk and surface study. *Phys Rev B*, 1999,59(16):10583–10590.
428. Bhandari C, Lambrecht WRL, van Schilfgaarde M. Quasiparticle self-consistent G W calculations of the electronic band structure of bulk and monolayer V₂O₅. *Phys Rev B*, 2015,91(12):125116.
429. Özgür Ü, Alivov YI, Liu C, Teke A, Reshchikov MA, Doğan S, et al. A comprehensive review of ZnO materials and devices. *J Appl Phys*, 2005,98(4):1–103.
430. Madelung O. *Semiconductors: Data Handbook*. Springer Berlin Heidelberg:

- Berlin, Heidelberg, 2004 doi:10.1007/978-3-642-18865-7.
431. Rezkallah T, Djabri I, Koç MM, Erkovan M, Chumakov Y, Chemam F. Investigation of the electronic and magnetic properties of Mn doped ZnO using the FP-LAPW method. *Chinese J Phys*, 2017,55(4):1432–1440.
 432. Aimouch DE, Meskine S, Cherif YB, Zaoui A, Boukortt A. Effect of sodium p-type doping on the structural, electrical and optical properties of zinc oxide. *Optik (Stuttg)*, 2017,130:1320–1326.
 433. Ahuja R, Eriksson O, Johansson B, Auluck S, Wills JM. Electronic and optical properties of red HgI₂. *Phys Rev B*, 1996,54(15):10419–10424.
 434. Ravindran P, Delin A, Ahuja R, Johansson B, Auluck S, Wills JM, et al. Optical properties of monoclinic SnI₂ from relativistic first-principles theory. *Phys Rev B*, 1997,56(11):6851–6861.
 435. Zhang S, Xie M, Cai B, Zhang H, Ma Y, Chen Z, et al. Semiconductor-topological insulator transition of two-dimensional SbAs induced by biaxial tensile strain. *Phys Rev B*, 2016,93(24):245303.
 436. Guo SD, Li HC. Monolayer enhanced thermoelectric properties compared with bulk for BiTeBr. *Comput Mater Sci*, 2017,139:361–367.
 437. Farzan M, Elahi SM, Salehi H, Abolhassani MR. An investigation of electronic and optical properties of InN nanosheet by first principle study. *Opt Commun*, 2017,395:293–300.
 438. Majidiyan Sarmazdeh M, Mendi RT, Mirzaei M, Motie I. Investigation of the electronic and optical properties of ZnS monolayer nanosheet: first principles calculations. *J Mater Sci*, 2017,52(6):3003–3015.
 439. Rahnamaye Aliabad HA, Asadi Rad F. Structural, electronic and thermoelectric properties of bulk and monolayer of Sb₂Se₃ under high pressure: By GGA and mBJ approaches. *Phys B Condens Matter*, 2018,545:275–284.
 440. Chen ZG, Hana G, Yanga L, Cheng L, Zou J. Nanostructured thermoelectric materials: Current research and future challenge. *Prog Nat Sci Mater Int*, 2012,22(6):535–549.
 441. Gao GY, Yao KL. Bulk and surface half-metallicity: Metastable zinc-blende TiSb. *J Appl Phys*, 2012,112(2):023712.
 442. Babamoradi M, Liyai MR, Azimirad R, Salehi H. Electronic structure and optical properties of the single crystal and two-dimensional structure of

- CdWO₄ from first principles. *Phys B Condens Matter*, 2017,511:103–108.
443. Zhou G, Wang D. Few-quintuple Bi₂Te₃ nanofilms as potential thermoelectric materials. *Sci Rep*, 2015,5(1):8099.
444. Maassen J, Lundstrom M. A computational study of the thermoelectric performance of ultrathin Bi₂Te₃ films. *Appl Phys Lett*, 2013,102(9):093103.
445. Mahmoodi T. A DFT Study on (001) Thin Slabs of SrTiO₃ and BaTiO₃. *Acta Phys Pol A*, 2015,127(6):1616–1620.
446. Aramberri H, Muñoz MC. Strain effects in topological insulators: Topological order and the emergence of switchable topological interface states in Sb₂Te₃ / Bi₂Te₃ heterojunctions. *Phys Rev B*, 2017,95(20):205422.
447. Acosta CM, Lima MP, da Silva AJR, Fazzio A, Lewenkopf CH. Tight-binding model for the band dispersion in rhombohedral topological insulators over the whole Brillouin zone. *Phys Rev B*, 2018,98(3):035106.
448. Weisbuch C, Vinter B. *Quantum semiconductor structures: fundamentals and applications*. Elsevier, 2014.
449. Dai J, Zeng XC. Bilayer phosphorene: Effect of stacking order on bandgap and its potential applications in thin-film solar cells. *J Phys Chem Lett*, 2014,5(7):1289–1293.
450. Gan ZX, Liu LZ, Wu HY, Hao YL, Shan Y, Wu XL, et al. Quantum confinement effects across two-dimensional planes in MoS₂ quantum dots. *Appl Phys Lett*, 2015,106(23):233113.
451. Zhang Y, Chang T, Zhou B, Cui Y, Yan H, Liu Z, et al. Direct observation of the transition from indirect to direct band gap in atomically-thin epitaxial MoSe₂. *Nat Nanotechnol*, 2014,9(2):111–115.
452. Sarmazdeh MM, Mendi RT, Zelati A, Boochani A, Nofeli F. First-principles study of optical properties of InN nanosheet. *Int J Mod Phys B*, 2016,30(19):1650117.
453. Khan SA, Azam S, Shah FA, Amin B. Electronic structure and optical properties of CdO from bulk to nanosheet: DFT approach. *Opt Mater (Amst)*, 2015,47:372–378.
454. Kumar A, Ahluwalia PK. Effect of quantum confinement on electronic and dielectric properties of niobium dichalcogenides NbX₂ (X = S, Se, Te). *J Alloys Compd*, 2013,550:283–291.
455. Dashora A, Ahuja U, Venugopalan K. Electronic and optical properties of

- MoS₂ (0001) thin films: Feasibility for solar cells. *Comput Mater Sci*, 2013,69:216–221.
456. Barbagiovanni EG, Lockwood DJ, Simpson PJ, Goncharova L V. Quantum confinement in Si and Ge nanostructures: Theory and experiment. *Appl Phys Rev*, 2014,1(1):011302.
457. Kondrotas R, Chen C, Tang J. Progress and Prospects of Sb₂S₃-Based Thin Film and Tandem Solar Cells. *Joule*, 2018,2(5):857–878.
458. Aousgi F, Dimassi W, Bessais B, Kanzari M. Effect of substrate temperature on the structural, morphological, and optical properties of Sb₂S₃ thin films. In: *Applied Surface Science*. North-Holland, 2015: 19–24.
459. Radzwan A, Ahmed R, Shaari A, Ng YXYX, Lawal A. First-principles calculations of the stibnite at the level of modified Becke–Johnson exchange potential. *Chinese J Phys*, 2018,56(3):1331–1344.
460. Radzwan A, Ahmed R, Shaari A, Lawal A, Ying Xuan Ng. First-principles calculations of antimony sulphide Sb₂S₃. *Malaysian J Fundam Appl Sci*, 2017,89(3):18–21.
461. Shahrokhi M, Leonard C. Quasi-particle energies and optical excitations of wurtzite BeO and its nanosheet. *J Alloys Compd*, 2016,682:254–262.
462. Hoat DM. Comparative study of structural, electronic, optical and thermoelectric properties of GaS bulk and monolayer. *Philos Mag*, 2018,;:1–16.
463. Li Y, Engheta N. Supercoupling of surface waves with ϵ -near-zero metastructures. *Phys Rev B*, 2014,90(20):201107.
464. Savoia S, Castaldi G, Galdi V, Alù A, Engheta N. PT-symmetry-induced wave confinement and guiding in ϵ -near-zero metamaterials. *Phys Rev B*, 2015,91(11):115114.
465. Fahrenbruch A, Bube R. *Fundamentals Of Solar Cells: Photovoltaic Solar Energy Conversion*. Elsevier, 2012 doi:10.1115/1.3267632.
466. Zhou Z, Zhao J, Chen Y, Schleyer P von R, Chen Z. Energetics and electronic structures of AlN nanotubes/wires and their potential application as ammonia sensors. *Nanotechnology*, 2007,18(42):424023.
467. Mohammad R, Katircioğlu Ş. First-principles calculations for mechanical and electronic features of strained GaP nanowires. *Int J Mod Phys C*, 2017,28(03):1750039.

468. Zhang Y, Wen Y-H, Zheng J-C, Zhu Z-Z. Direct to indirect band gap transition in ultrathin ZnO nanowires under uniaxial compression. *Appl Phys Lett*, 2009,94(11):113114.
469. Khuili M, Fazouan N, Makarim HA El. DFT study of physical properties of wurtzite, zinc blende, and rocksalt phases of zinc oxide using GGA and TB-mBJ potential. In: *2015 3rd International Renewable and Sustainable Energy Conference (IRSEC)*. IEEE, 2015: 1–4.
470. John R, Padmavathi S. Ab Initio Calculations on Structural, Electronic and Optical Properties of ZnO in Wurtzite Phase. *Cryst Struct Theory Appl*, 2016,05(02):24–41.
471. Zhao X, Wei CM, Yang L, Chou MY. Quantum Confinement and Electronic Properties of Silicon Nanowires. *Phys Rev Lett*, 2004,92(23):236805.
472. Leu PW, Shan B, Cho K. Surface chemical control of the electronic structure of silicon nanowires: Density functional calculations. *Phys Rev B*, 2006,73(19):195320.
473. Naseri M, Lin S, Jalilian J, Gu J, Chen Z. Penta-P2X (X=C, Si) monolayers as wide-bandgap semiconductors: A first principles prediction. *Front Phys*, 2018,13(3):138102.
474. Leu PW, Svizhenko A, Cho K. *Ab initio* calculations of the mechanical and electronic properties of strained Si nanowires. *Phys Rev B*, 2008,77(23):235305.
475. Yu H, Li J, Loomis RA, Wang L-W, Buhro WE. Two- versus three-dimensional quantum confinement in indium phosphide wires and dots. *Nat Mater*, 2003,2(8):517–520.
476. Anasthasiya ANA, Ramya S, Balamurugan D, Rai PK, Jeyaprakash BG. Adsorption property of volatile molecules on ZnO nanowires: computational and experimental approach. *Bull Mater Sci*, 2018,41(1):4.
477. Zhang A, Liu W, Zhang Y. Piezoelectricity and electronic structures of ZnO thin films: A density functional theory study. *Surf Sci*, 2015,642:45–50.
478. Kang Y-G, Kim S-W, Cho J-H. Competing charge density wave and antiferromagnetism of metallic atom wires in GaN($10 \times 1 \times 0$) and ZnO($10 \times 1 \times 0$). *Phys Rev B*, 2017,96(23):235416.
479. Wang B, Yin S, Wang G, Buldum A, Zhao J. Novel Structures and Properties of Gold Nanowires. *Phys Rev Lett*, 2001,86(10):2046–2049.

480. Srivastava A, Tyagi N, Ahuja R. First-principles study of structural and electronic properties of gallium based nanowires. *Solid State Sci*, 2013,23:35–41.
481. Li Y, Bai H, Li L, Huang Y. Stabilities and electronic properties of nanowires made of single atomic sulfur chains encapsulated in zigzag carbon nanotubes. *Nanotechnology*, 2018,29(41):415703.
482. Nayebi P, Emami-Razavi M, Zaminpayma E. Electronic and optical properties of CuGaS₂ nanowires: a study of first principle calculations. *Eur Phys J B*, 2017,90(1):11.
483. Song X, Zhou W, Liu X, Gu Y, Zhang S. Layer-controlled band alignment, work function and optical properties of few-layer GeSe. *Phys B Condens Matter*, 2017,519:90–94.
484. Adachi MM, Khorasaninejad M, Saini SS, Karim KS. Optical Properties of Silicon Nanowires. In: *UV-VIS and Photoluminescence Spectroscopy for Nanomaterials Characterization*. Springer Berlin Heidelberg: Berlin, Heidelberg, 2013: 357–385.
485. BP Pandey. Electronic and Optical Properties of GaAs Armchair Nanoribbons: DFT Approach. *Int J Nanoelectron Mater*, 2018,11(2):143–152.
486. Davelou D, Kopidakis G, Kioseoglou G, Remediakis I. MoS₂ nanostructures: Semiconductors with metallic edges. *Solid State Commun*, 2014,192:42–46.
487. Valedbagi S, Jalilian J, Elahi SM, Majidi S, Fathalian A, Dalouji V. Ab initio calculations of electronic and optical properties of BeO nanosheet. *Electron Mater Lett*, 2014,10(1):5–11.
488. Ma Y, Dai Y, Guo M, Yu L, Huang B. Tunable electronic and dielectric behavior of GaS and GaSe monolayers. *Phys Chem Chem Phys*, 2013,15(19):7098–7105.

LIST OF PUBLICATIONS

1. **Radzwan, A.**, Ahmed, R., Shaari, A., Lawal, A. and Ng, Y.X., (2017). First-principles calculations of antimony sulphide Sb₂S₃. *Malaysian Journal of Fundamental and Applied Sciences*, 13(3), 285-289. <https://doi.org/10.11113/mjfas.v13n3.598>
2. **Radzwan, A.**, Ahmed, R., Shaari, A., Ng, Y. X., & Lawal, A. (2018). First-principles calculations of the stibnite at the level of modified Becke–Johnson exchange potential. *Chinese Journal of Physics*, 56(3), 1331-1344. <https://doi.org/10.1016/j.cjph.2018.03.005> (Q3, IF: 1.051)
3. **Radzwan, A.**, Ahmed, R., Shaari, A. and Lawal, A., (2019). Ab initio calculation of antimony sulphide nanowire. *Physica B: Condensed Matter*. 557, 17-22. <https://doi.org/10.1016/j.physb.2019.01.005> (Q3, IF: 1.453)
4. **Radzwan, A.**, Ahmed, R., Shaari, A. and Lawal, A., (2019). Ab initio calculations of optoelectronic properties of antimony sulfide nano-thin film for solar cell applications. *Results in Physics*, 15, 102762. <https://doi.org/10.1016/j.rinp.2019.102762>
5. **Radzwan, A.**, Ahmed, R., Shaari, A. and Lawal, A., (2020). First-principles study of electronic and optical properties of antimony sulphide thin film. *Optik*, 202, 163631. <https://doi.org/10.1016/j.ijleo.2019.163631>